FAA-RD-74-4

Project Report
ATC-20

The Effects of ATCRBS P2 Pulses on DABS Reliability

W. H. Harman
D. A. Shnidman

28 January 1974

Lincoln Laboratory
MASSACHUSETTS INSTITUTE OF TECHNOLOGY
LEXINGTON, MASSACHUSETTS

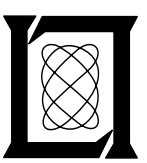

Prepared for the Federal Aviation Administration,
Washington, D.C. 20591

This document is available to the public through
the National Technical Information Service,
Springfield, VA 22161

TECHNICAL REPORT STANDARD TITLE PAGE

1. Report No.	2. Government Accession No.	3. Recipient's Catalog No.
FAA-RD-74-4		

4. Title and Subtitle	5. Report Date
The Effects of ATCRBS P_2 Pulses on DABS Reliability	28 January 1974
	6. Performing Organization Code

7. Author(s)	8. Performing Organization Report No.
W.H. Harman and D.A. Shnidman	ATC-20

9. Performing Organization Name and Address	10. Work Unit No. (TRAIS) 45364
Massachusetts Institute of Technology Lincoln Laboratory P.O. Box 73 Lexington, Massachusetts 02173	Proj. No. 034-241-012
	11. Contract or Grant No. IAG-DOT-FA72 WAI-261
	13. Type of Report and Period Covered Project Report
12. Sponsoring Agency Name and Address Department of Transportation Federal Aviation Administration Systems Research and Development Service Washington, D.C. 20591	14. Sponsoring Agency Code

15. Supplementary Notes

The work reported in this document was performed at Lincoln Laboratory, a center for research operated by Massachusetts Institute of Technology under Air Force Contract F19628-73-C-0002.

16. Abstract

An analytical study is performed to determine the effects of ATCRBS P_2 pulses as interference to DABS uplink transmissions. These effects constitute a major component of all uplink error-producing mechanisms that are anticipated to occur in DABS operation.

The study is formulated in a way that includes effects of both receiver noise and P_2 pulse interference, where the interference can be received from any of a number of different transmitters at different distances from the receiving aircraft. The model includes the randomness associated with whether or not a particular DABS signal is overlapped by any interference pulse, and also the conditional randomness of error production given that an overlap does occur. In fact, a major portion of the study is the determination of the conditional error probability given the occurrence of an overlap with stated signal-to-interference ratio and stated signal-to-noise ratio.

The results are given as the probability of a "miss," where a "miss" is the event that at least one of the bits in the DABS data block is demodulated in error. The study is carried out for both DPSK and PAM which are the two modulation options being considered in the DABS design. Results are given both as general formulas and as evaluations of these formulas in various specific cases. In these evaluations, the interference environment is based on ATCRBS interrogator locations, transmitter powers, and repetition frequencies as listed in ECAC's IFF Master File. The numerical results are presented graphically to display the dependence on signal level, noise level, and geographical location between Boston and Washington, D.C. A concept referred to as "effective interference tolerance" is introduced, and numerical evaluations are presented to indicate the accuracy of this concept.

17. Key Words		18. Distribution Statement
DABS	DPSK	Document is available to the public through the National Technical Information Service, Springfield, Virginia 22151
ATCRBS	PAM	
Interference		
Modulation		
SLS		

19. Security Classif. (of this report)	20. Security Classif. (of this page)	21. No. of Pages	22. Price
Unclassified	Unclassified	68	3.50

Form DOT F 1700.7 (8-69)

TABLE OF CONTENTS

LIST OF ILLUSTRATIONS

LIST OF TABLES

1. INTRODUCTION AND SUMMARY

1.1 Introduction

As presently envisioned, the DABS* uplink signal will be in the 1030 MHz frequency band and will consist of a "preamble" followed by a "data block." The data block is a stream of binary information, containing approximately 100 bits, modulated as either PAM (pulse amplitude modulation) or DPSK (differential phase shift keying). The bits represent aircraft address plus additional information, all protected by an error detection code. The purpose of this report is to evaluate the probability of an error occurring in the data block due to pulse interference produced by ATCRBS* interrogators (which also operate in the 1030 MHz frequency band). In particular, attention is limited to P_2 pulses as the only type of interference considered.**

The study has been limited in this particular way for two reasons: (1) that the effect considered appears to be the dominant error mechanism, and (2) that so limiting the scope of the problem simplifies a very complex situation

*"DABS" denotes the Discrete Address Beacon System, an air traffic control sensor system now being designed, for use in the future. "ATCRBS" denotes the Air Traffic Control Radar Beacon System, an existing sensor for air traffic control.

**Ref. [1] gives an introductory description of ATCRBS with an explanation of what P_2 pulses are and how they are transmitted.

making it far more manageable for analysis and making the results and underlying phenomena far more understandable. Concerning the claim that the P_2-to-data-block effect is dominant, it is pointed out in Ref. [2] that the arrival rate of P_2 pulses in a 1030 MHz aircraft receiver is considerably greater than arrival rates of interrogations and suppressions. This property may be expected to hold at most altitudes, geographical locations, and receiver sensitivities of interest. Taking this property together with the fact that the DABS data block is considerably longer than the preamble (by about 5:1), leads one to the conclusion referred to above as (1). A more detailed comparison between the various DABS uplink error mechanisms will be carried out in a later report.

The model upon which this study is based is diagrammed in Figure 1. The model includes effects of noise as well as interference, and includes the property that the interference may come from a collection of transmitters, each having a different received power level and a different repetition frequency. Effects of intersymbol interference* and imperfect bit synchronization are not included. The following parameters are referred to in the figure,

T_b = duration of DABS data block

n = number of bits

K = number of interference sources

τ = width of an interference pulse

SIR_k = signal-to-interference ratio of the k^{th} interferer

f_k = repetition frequency of the k^{th} interferer

and certain constraints among these parameters are stated there. The constraint $\tau \approx 3T_b/n$ is a generalization of τ = 0.8 μsec and chip duration = 0.25 μsec,

*"Intersymbol interference" refers to interference to a bit from time - adjacent bits.

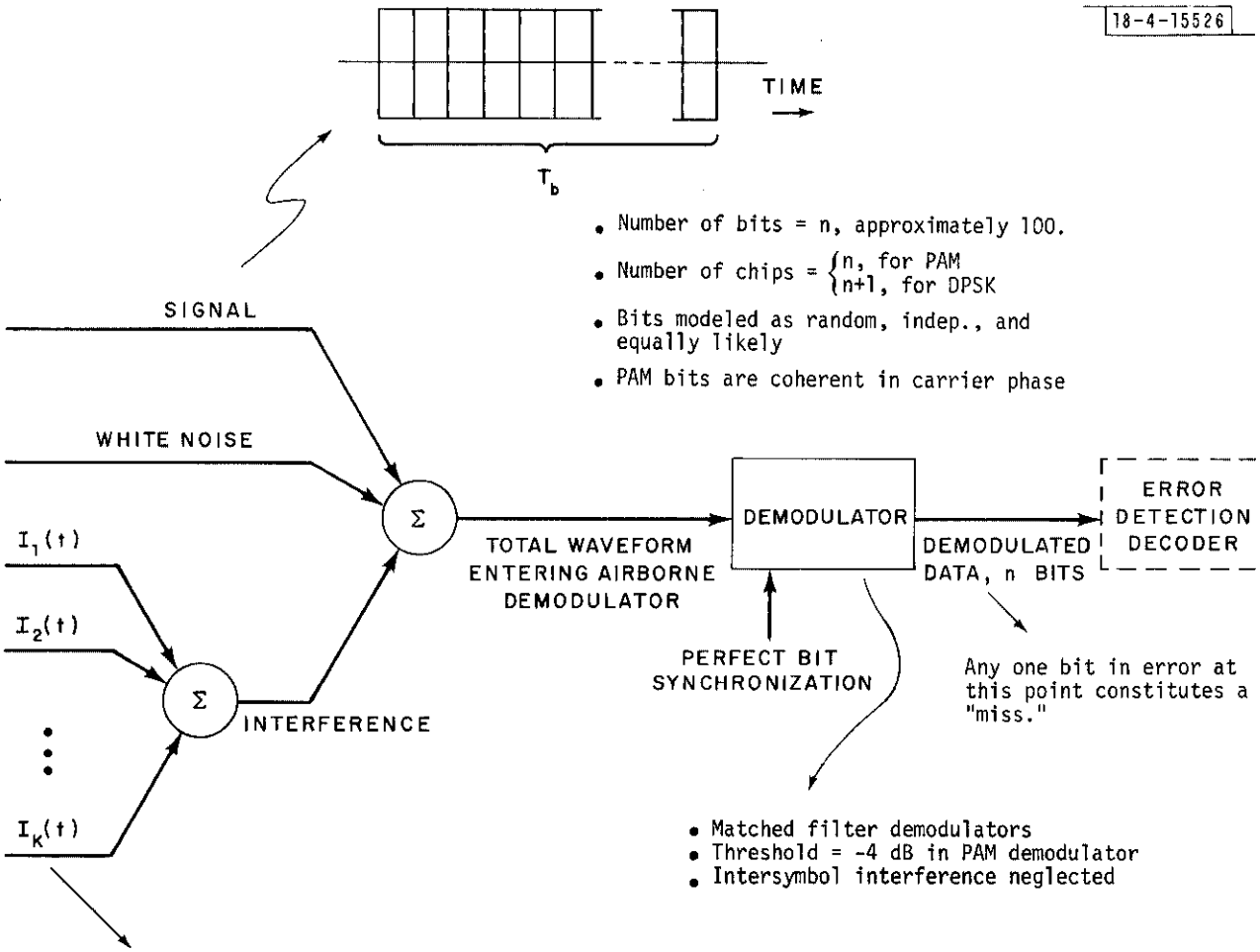

Properties of the interference: for each k = 1,2,...K, $I_k(t)$ is a periodic train of rectangular pulses with

- pulse width = τ (indep. of k, constrained to satisfy $\tau \approx 3T_b/n$)
- repetition frequency = f_k (a function of k, constrained to not exceed about $f_k \approx 0.01/T_b$)
- signal-to-interference ratio = SIR_k (a function of k, defined as the ratio of powers in the "on" state)

Also, the collection of interferences satisfies

- carrier frequencies -- all equal to the signal frequency
- carrier phases -- random, indep. of the signal, indep. of each other, uniformly distributed
- pulse repetition phases -- random, indep. of the signal, indep. of each other, uniformly distributed
- K does not exceed about 100

Fig. 1. Model Used for Analyzing the P_2-to-Data-Block Effect.

which are typical values of interest. A "miss" is defined as the event that at least one bit is demodulated in error.

As indicated in Figure 1, the study is applicable to noncoherent matched-filter demodulators. Figure 2 illustrates possible configurations of these demodulators.

1.2 Summary of Results

The following formula is derived for miss probability, P(miss).

$$P(\text{miss}) = 1 - (1 - p)^n \, e^{-(T_b+\tau) \sum_{k=1}^{K} f_k \, P'(M/\Omega;\ SIR_k,\ SNR)} \qquad (1\text{-}1)$$

where

p = bit error probability in noise alone

SNR = signal-to-noise ratio

and $P'(M/\Omega;\ SIR_k,\ SNR)$ is the conditional probability of at least one error occurring in the bits overlapped given that an interference pulse overlaps the data block with signal-to-interference ratio of SIR_k. Evaluations of p as a function of SNR have been developed previously, for example in Ref. [3]. Signal-to-noise ratio SNR is defined as

$$SNR = \frac{E}{N_o}$$

where E is the signal energy per bit and N_o is the one-sided noise power density.

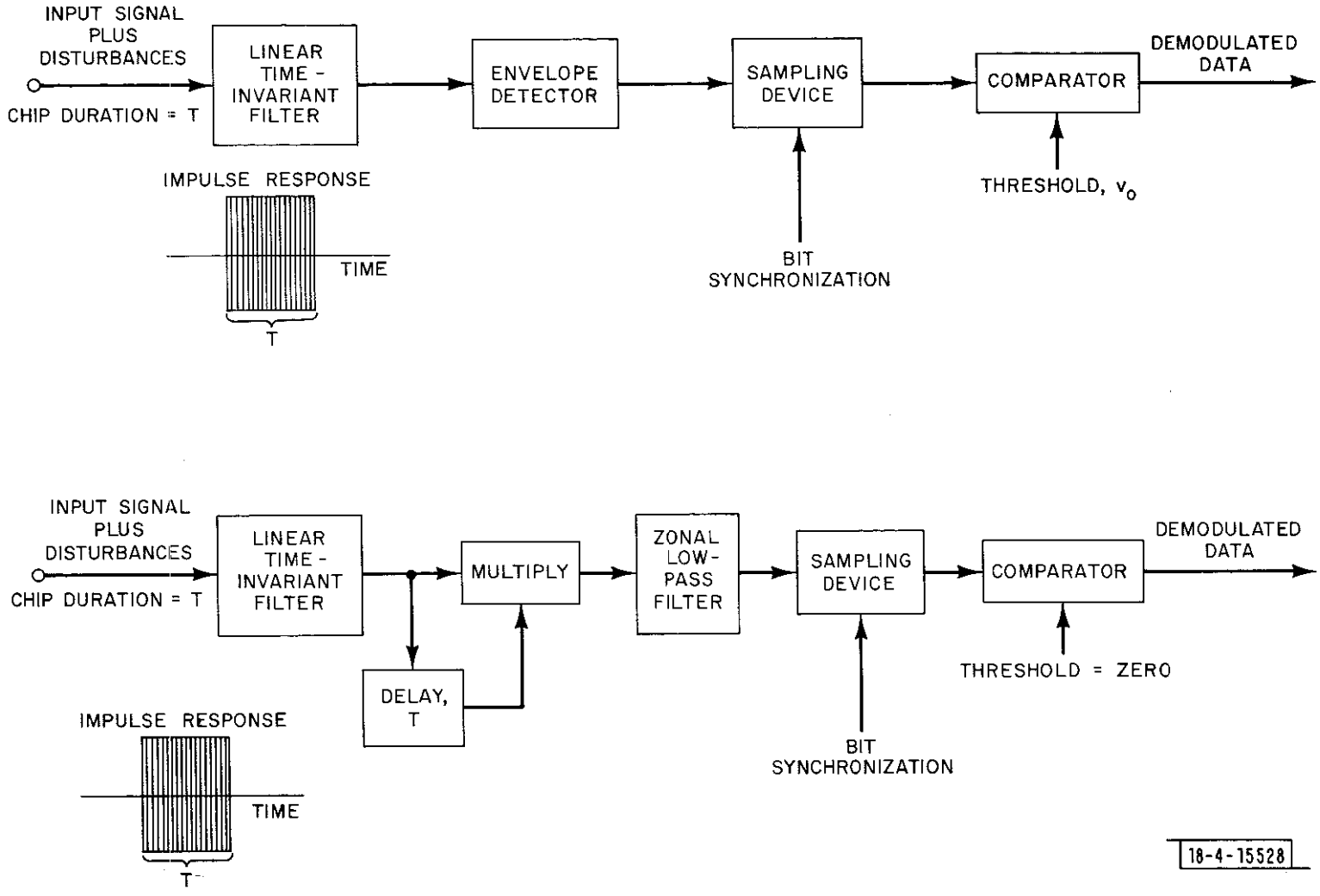

Figure 2. Non-coherent Matched Filter Demodulators for PAM and DPSK.

In the following sections, explicit formulas for $P'(M/\Omega; SIR, SNR)$ are derived. They are extremely lengthy. Computer evaluations have been carried out, and results of these are presented graphically showing P' as a function of SIR for both types of modulation and for several values of SNR.

Using these results together with data describing the interference environment, computer evaluations of P(miss) according to Eq. (1-1) were carried out. The interference environment is characterized by

$$\{f_1, f_2, \ldots f_K\} = \text{set of repetition frequencies}$$
$$\{SIR_1, SIR_2, \ldots SIR_K\} = \text{set of signal-to-interference ratios}$$

These data are obtained from ECAC's IFF Master File,* used with a simplified calculation of received power from each interrogator (free-space path loss within 4/3-earth line-of-sight, omnidirectional aircraft antenna). Results of the P(miss) evaluations are presented graphically in various ways to display the dependence on signal power level, the dependence on geographical location, and the dependence on SNR.

Examination of formulas and graphs has suggested a simple rule of thumb by which to characterize the interference-error mechanism. The suggestion is that both DPSK and PAM be thought of as having an "effective interference tolerance" described by an effective SIR level required for error-free reception. The effective SIR, denoted SIR_e is given the values

*The IFF Master File is a listing of ATCRBS interrogators and their characteristics, maintained by ECAC (Electromagnetic Compatability Analysis Center).

$$SIR_e = \begin{cases} 0 \text{ dB}, & \text{DPSK} \\ 6 \text{ dB}, & \text{PAM} \end{cases}$$

(for matched-filter demodulators) with the property that interference of lesser power never causes an error and interference of greater power always causes an error. Whereas this simple rule is not strictly correct, it does provide an easy-to-use approximation that is found to be reasonably accurate.

1.3 Effects Not Considered

It should not be forgotten that many effects are not considered in this study. For example, in actuality many interrogators employ some sort of pulse stagger instead of strictly periodic transmissions. Also, multipath reflections can in some cases produce additional received pulses. Furthermore, a broad range of idealizations has been used in obtaining the interference-environment data (such as neglecting terrain and man-made obstructions and propagation anomalies).

As indicated in Figure 1, this study is limited to ideal demodulators and thus neglects any effects of imperfect bit synchronization, mismatched filtering, and intersymbol interference. However, examining the derivation of Eq. (1-1) suggests that this equation would still be accurate if these idealizations were relaxed, provided that the appropriate P'(M/Ω; SIR, SNR) were inserted. This P' data could be obtained from analysis, laboratory measurement, or simulation. In fact, Ref. [4] presents simulation results of P' for the case of PAM with a second-order filter instead of a perfect matched filter. Interestingly, the simulation results agree quite well with the P' results obtained in this study.

Another category of effects not considered here results from the limitation to the relationship between P_2 pulses and the DABS data block. Yet to be evaluated are the effects of P_2 pulses on the DABS preamble and the effects of the other interference pulses (P_1 and P_3) on both data block and preamble.

As was stated in Section 1.1, these idealizations are set up deliberately in this study in order to allow an in-depth investigation of a single effect of primary importance.

2. EXPRESSIONS USED IN DETERMINING UPLINK RELIABILITY

Expressions used to determine uplink reliability are summarized in this section. Derivations are given in Appendix A.

In previous sections we have denoted by $P'(M/\Omega; SIR, SNR)$ the conditional probability of a miss with an error occurring in the bits overlapped given that an interference pulse overlaps the data block. To simplify notation we define

$$\rho = \frac{1}{\sqrt{SIR}}$$

and

$$\gamma = \sqrt{SNR} \quad .$$

The following expressions for conditional miss probability P' apply to the specific case

P2-pulse duration, τ, = 0.8 μsec

chip duration, T, = 0.25 μsec

and are approximations, sufficiently accurate for our purposes.

For DPSK the result is

$$P'(M/\Omega;\ 1/\rho^2,\ \gamma^2)$$

$$= \frac{1}{5}\left\{1 - \frac{1}{2\pi}\int_{-\pi}^{\pi}\left[1 - \frac{1}{2}\left\{P_e(\gamma,\rho,\rho,\theta) + P_e(\gamma,\rho,-\rho,\theta)\right\}\right]^2 \right.$$

$$\times\left[1 - \frac{1}{2}\left\{P_e\left(\gamma,\rho,\sqrt{\frac{1}{10}}\,\rho,\theta\right) + P_e\left(\gamma,\rho,-\sqrt{\frac{1}{10}}\,\rho,\theta\right)\right\}\right]^2$$

$$\left.\times\left[1 - P_e\left(\gamma,\sqrt{\frac{1}{10}}\,\rho,0,\theta\right)\right]^2 d\theta\right\}$$

$$+ \frac{4}{5}\left\{1 - \frac{1}{2\pi}\int_{-\pi}^{\pi}\left[1 - \frac{1}{2}\left\{P_e(\gamma,\rho,\rho,\theta) + P_e(\gamma,\rho,-\rho,\theta)\right\}\right]\right.$$

$$\times\left[1 - \frac{1}{2}\left\{P_e\left(\gamma,\rho,\sqrt{\frac{3}{5}}\,\rho,\theta\right) + P_e\left(\gamma,\rho,-\sqrt{\frac{3}{5}}\,\rho,\theta\right)\right\}\right]^2$$

$$\left.\times\left[1 - P_e\left(\gamma,\sqrt{\frac{3}{5}}\,\rho,0,\theta\right)\right]^2 d\theta\right\} \qquad (2\text{-}1)$$

where

$$P_e(\gamma,\ \rho_1,\ \rho_2,\ \theta) = \frac{1}{2}\left[1 - Q(\sqrt{b},\ \sqrt{a}) + Q(\sqrt{a},\ \sqrt{b})\right]$$

$$a = 2\gamma^2\left(\frac{\rho_1 - \rho_2}{2}\right)^2$$

$$b = 2\gamma^2\left[1 + 2\left(\frac{\rho_1 + \rho_2}{2}\right)\cos\theta + \left(\frac{\rho_1 + \rho_2}{2}\right)^2\right] \quad .$$

and Q is the Mareum Q function.

For PAM, the result depends on the threshold level used in the demodulator, expressed by a parameter v_o. If we let α denote the ratio of the actual threshold level to the noise-free and interference-free sampled output of the receiver, then v_o is defined as

$$v_o = \alpha\gamma\sqrt{2} \quad .$$

In terms of v_o the PAM result is

$$P'(M/\Omega;\ 1/\rho^2,\gamma^2)$$

$$= \frac{1}{5}\left\{1 - \frac{1}{2\pi}\int_{-\pi}^{\pi}\left[1 - \frac{1}{2}\left\{Q\left(\rho\gamma\sqrt{2},\ v_o\right) + 1 - Q(R[\rho,\theta],\ v_o)\right\}\right]^3\right.$$

$$\left. \times \left[1 - \frac{1}{2}\left\{Q\left(\rho\gamma\sqrt{\frac{1}{5}},\ v_o\right) + 1 - Q\left(R\left[\sqrt{\frac{1}{10}}\,\rho,\theta\right],\ v_o\right)\right\}\right]^2 d\theta\right\}$$

$$+ \frac{4}{5}\left\{1 - \frac{1}{2\pi}\int_{-\pi}^{\pi}\left[1 - \frac{1}{2}\left\{Q\left(\rho\gamma\sqrt{2},\ v_o\right) + 1 - Q(R[\rho,\theta],\ v_o)\right\}\right]^2\right.$$

$$\left. \times \left[1 - \frac{1}{2}\left\{Q\left(\rho\gamma\sqrt{\frac{6}{5}},\ v_o\right) + 1 - Q\left(R\left[\sqrt{\frac{3}{5}}\,\rho,\theta\right],\ v_o\right)\right\}\right]^2 d\theta\right\}$$

(2-2)

where

$$R[\rho,\theta] = \sqrt{2\gamma^2(1 + 2\rho \cos \theta + \rho^2)} \quad .$$

In addition, analogous expressions for the noise free cases are derived in Appendix A. The expression for DPSK is given by (A-31) and for PAM by (A-35).

It is further shown (in Appendix A, Section A.1) that the unconditional probability of a miss can be expressed for our purposes in terms of P'(M/Ω; SIR, SNR) by Eq. (1-1).

3. RESULTS

3.1 Evaluation of Conditional Miss Probabilities

We wish to evaluate the conditional miss probabilities as expressed by Eq. (2-1) and Eq. (2.2). For DPSK we use the values

$$20 \log \gamma = 10 \log \text{SNR} = 10, 20, 30 \text{ dB}$$

$$20 \log \rho = -10 \log \text{SIR} = -12, -8, -7, -6, -5, -4, -2, -1, 0, 2, 4, 10 \text{ dB}.$$

The results are tabulated in Table 3.1.

For PAM, we evaluate $P'(M/\Omega;\ 1/\rho^2, \gamma^2)$ for $v_0 = 0.893\ \gamma$ ("a -4dB threshold") and

$$20 \log \gamma = 10 \log \text{SNR} = 16, 26, 36 \text{ dB}$$

$$20 \log \rho = -10 \log \text{SIR} = -12, -8, -6, -4.2, -4, -3.8, -1, 1, 3, 10 \text{ dB}.$$

The results are presented in Table 3.2.

In Tables 3.3 and 3.4 the noise free evaluation are given for DPSK and PAM, respectively (based on formulas in Appendix A). The $\rho \to \infty$ asymptotes from these tables have been included in the two previous tables.

Since it is necessary to use the conditional probability of miss at values of ρ other than those calculated, an interpolation is done which yields value for all ρ. The functions used fit the tabulated data and have sufficient smoothness for our purposes. They are shown in Figure 3 and given in Appendix C.

Table 3.1. Evaluation of $P'(M/\Omega; 1/\rho^2, \gamma^2)$ for DPSK.

Interference-to-Signal Ratio, ρ^2 (dB)	Signal-to-Noise Ratio, γ^2 (dB)		
	10	20	30
-12	0.00128		
-8	0.00782		
-7	0.01356		
-6	0.02416		
-5	0.04376		
-4	0.07941		
-2	0.2385	0.00188	
-1	0.3741	0.06162	5.18×10^{-7}
0	0.5315	0.4276	0.3873
2	0.7825	0.8199	0.8614
4	0.8722	0.8739	0.8725
10	0.9294	0.9283	0.9292
∞	0.971875	0.971875	0.971875

Table 3.2. Evaluation of $P'(M/\Omega; 1/\rho^2, \gamma^2)$ for PAM.

Interference-to-Signal Ratio, ρ^2 (dB)	Signal-to-Noise Ratio, γ^2 (dB)		
	16	26	36
-12	0.0326	3.28×10^{-5}	$< 10^{-12}$
-8	0.145	0.0833	0.078
-6	0.323	0.155	0.148
-4.2	0.630	0.507	0.296
-4	0.665	0.619	0.616
-3.8	0.699	0.713	0.821
-1	0.914	0.926	0.927
1	0.928	0.926	0.924
3	0.928	0.922	0.921
10	0.957	0.957	0.957
∞	0.94375	0.94375	0.94375

Table 3.3. Noise Free Probabilities of Miss for DPSK.

ρ (dB)	$P'(M/\Omega;\ 1/\rho^2,\ \infty)$
<0	0
0	0.3625
1	0.7386
2	0.8086
4	0.8590
10	0.9291
∞	0.971875

Table 3.4. Noise Free Probabilities of Miss for PAM.

ρ (dB)	$P'(M/\Omega;\ 1/\rho^2,\ \infty)$
-12	0
-8	0.078
-6	0.143
-4^-	0.295
-4^+	0.852
-1	0.926
1	0.924
3	0.921
5	0.922
10	0.947
∞	0.94375

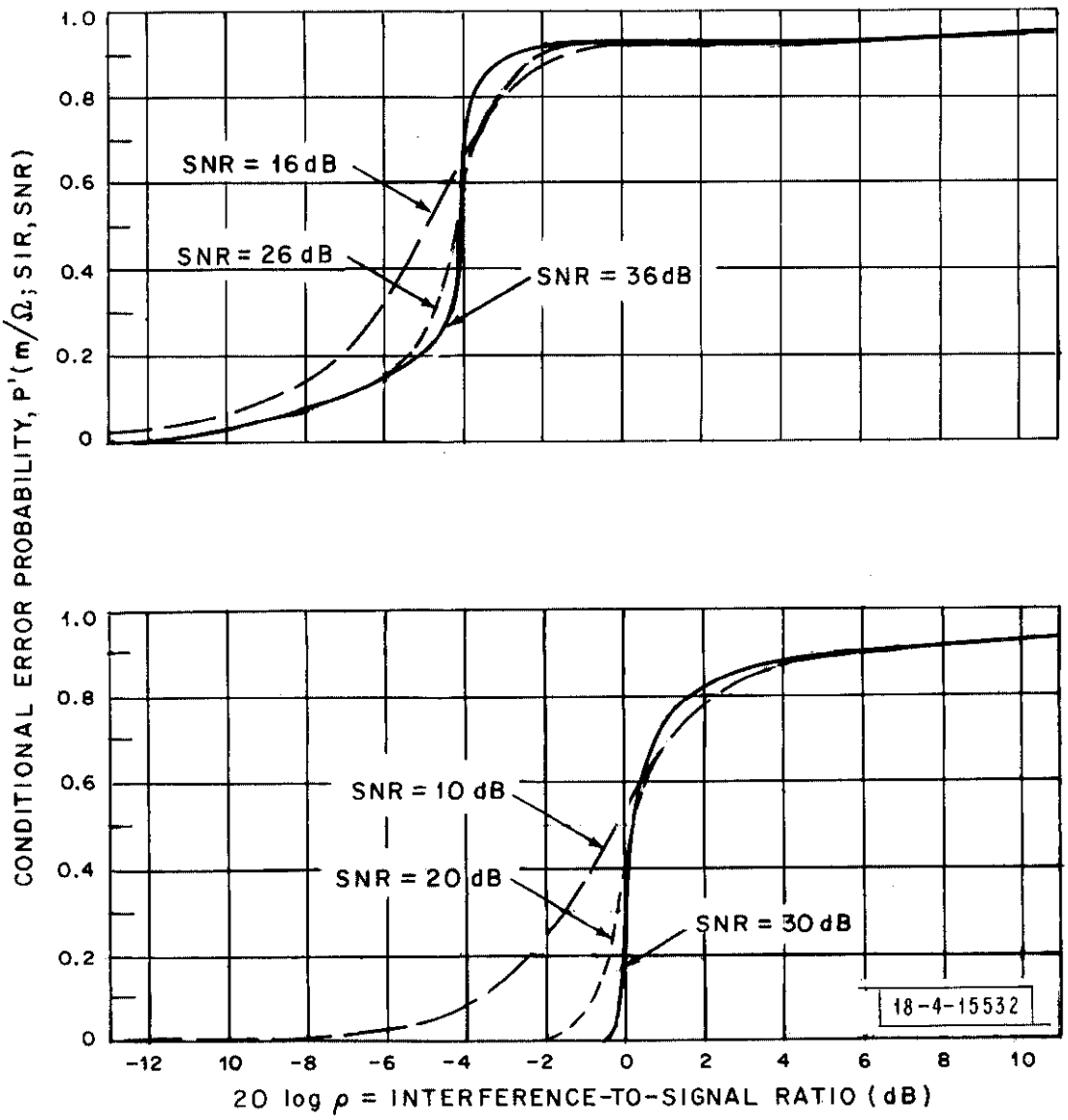

Fig. 3. Conditional Miss-Probability Curves.

(a) PAM with threshold at -4 dB.

(b) DPSK.

Note: Analytical results for matched filter demodulators, τ=0.8 μsec, chip duration = 0.25 μsec, n = 100 bits.

3.2 Evaluation of Miss Probabilities

In this section, evaluation of P(miss) is carried out by combining data describing the interference environment with the conditional miss probabilities evaluated in the previous section. Computer calculations are employed making use of a subroutine for the conditional miss probability, which subroutine executes the interpolation formulas given in Appendix C.

The interference environment data are based on the 1972 IFF Master File (Ref. [2]). To represent future conditions, it is assumed that all interrogators are equipped with ISLS or IISLS* and therefore all transmit P_2 pulses. In addition, the following assumptions are made in calculating power received from each interrogator.

- Received power = $I = P_t L_t G_t L_p G_r L_r$.
- Transmitter power = P_t = that given in the IFF Master File.
- Transmitter coupling loss = L_t = - 3 dB.
- Transmitting antenna gain = G_t = 4 dB.
- Path loss = L_p = free space path loss, $\lambda^2/(4\pi R_s)^2$, where λ is wavelength and R_s is slant range, for points satisfying 4/3 earth line-of-sight; zero otherwise.
- Slant range = $R_s = \sqrt{R_g^2 + h^2}$, where R_g is ground range and h is altitude.
- Ground range = $R_g = (\frac{60 \text{ nmi}}{\text{degree}})$ Arc cos C where

*ISLS (interrogator sidelobe suppression) and IISLS (improved interrogator sidelobe suppression) are described in Ref. [1].

$C = \sin \lambda_1 \sin \lambda_2 + \cos \lambda_1 \cos \lambda_2 \cos(L_2 - L_1)$,

λ_1, λ_2 = latitudes of the transmitter and receiver respectively,

L_1, L_2 = longitudes of the transmitter and receiver respectively,

which is the great-circle distance between two points on a sphere.

- Receiving antenna gain = G_r = + 2 dB.
- Receiving coupling loss = L_r = - 3 dB.

This interference calculation is carried out to obtain the interference environment in the form f_1, f_2, ... f_K and SIR_1, SIR_2, ... SIR_K for direct use in Eq. (1-1). The interference environment can conveniently be displayed in its own right in the form shown in Figure 4. The graphs show the cumulative power distribution of the P_2 arrival rate, denoted PAR. That is

$$PAR(I) = \sum_{k=1}^{K} f_k \, u(I_k - I) \qquad (3\text{-}1)$$

where I_k is the received power from the k^{th} interferer and

$$u(x) = \begin{cases} 1 & \text{for} \quad x \geq 0 \\ 0 & \text{for} \quad x < 0 \end{cases} . \qquad (3\text{-}2)$$

The graph shows both "nominal" and "maximum" environments, which are terms used to indicate

nominal environment -- a subset of interrogators including only those which operate at least 33% of the time.

maximum environment -- all interrogators.

18-4-15533

AIRCRAFT COORDINATES

	LATITUDE (N)	LONGITUDE (W)	ALTITUDE (ft)
NEW YORK	40d, 38m, 11s	73d, 46m, 03s	10,000
PHILADELPHIA	39d, 52m, 32s	75d, 14m, 01s	10,000
LOS ANGELES	33d, 57m, 14s	118d, 24m, 28s	10,000

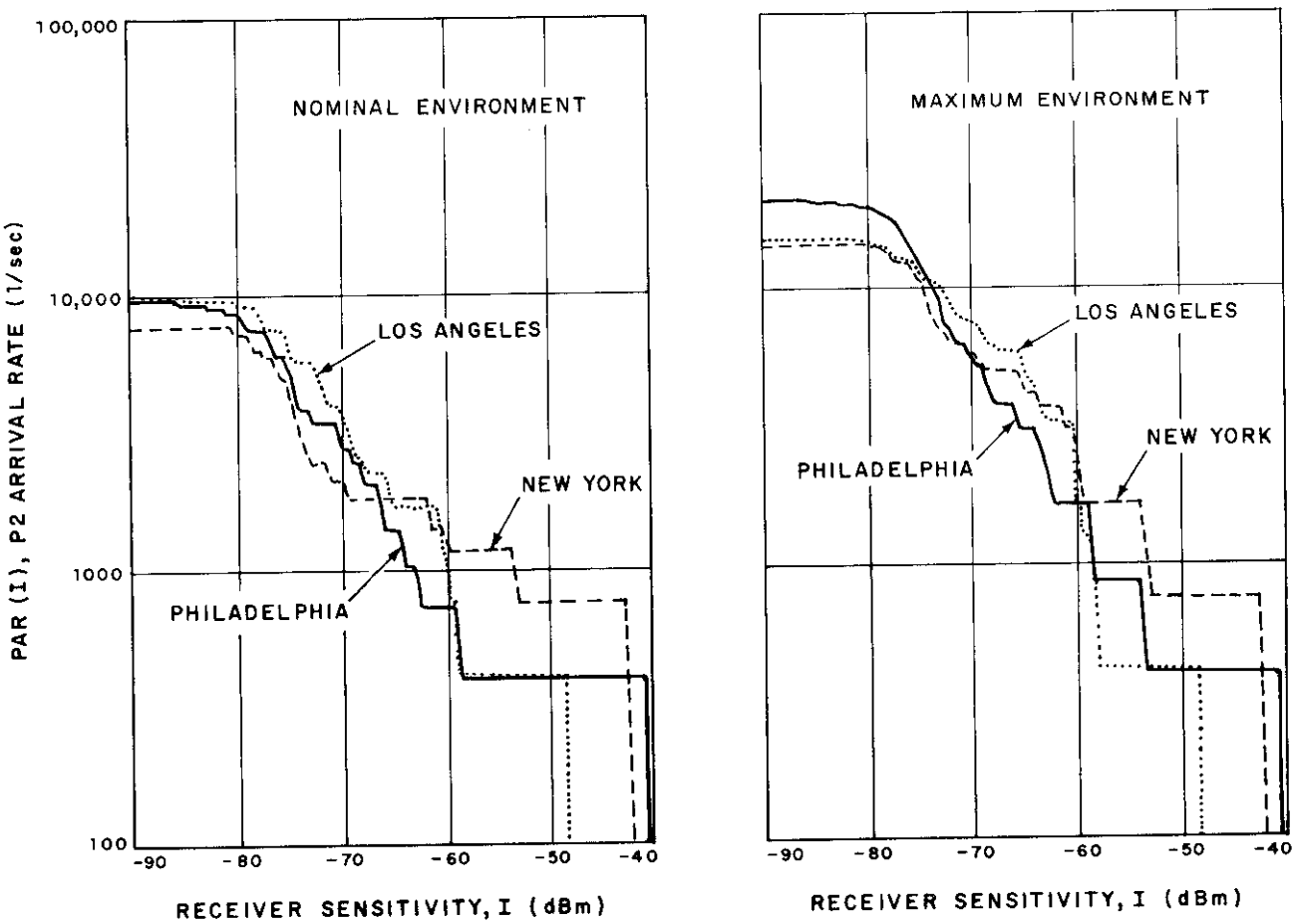

Fig. 4. Interference Environment Illustrated by the P_2 Arrival Rate.

Note: PAR(I) = Arrival rate of P_2 pulses having power $\geq$ I.

The results obtained in evaluating P(miss) are plotted in Figures 5, 6, and 7. Figure 5 shows the dependence on received signal power, with aircraft location and noise level taken to be constant. Figure 6 shows the dependence on geographical location of the aircraft along a contour between Boston and Washington, D.C., with signal level, noise level, and altitude held constant. The contour is described as a function of x by

$$\text{latitude} = (42,25,00) - x(03,35,00)$$

$$\text{longitude} = (71,00,00) + x(06,00,00)$$

where x=0 at Boston and x=1 at Washington. The triplet notation used here denotes (degrees, minutes, seconds). A map of the geographical area showing this contour is given in Figure 8. The dependence on noise level is shown in Figure 7 for fixed location and fixed signal strength.

The data in Figure 7 indicate that results are not particularly sensitive to noise level, especially in the case of PAM. This behavior can be related to the curve shapes shown in Figure 3; as noise level is increased, the curves tend to flatten out in a way that produces degradation in some regions and improvement in others. Evidently, the two effects tend to cancel making P(miss) rather insensitive to noise level.

The geographical dependence data of Figure 6 reflects to some extent the concentrations of interrogators around Boston, New York, and Washington. Whereas the DPSK data tends to peak up separately around New Jersey and Washington, the PAM data reaches a single peak value midway between -- somewhat south of Philadelphia. This behavior is probably due to the differing sensitivities to interference of the two types of modulation. Under these conditions (signal at -70 dBm), PAM may be sensitive to interference coming from as far away as

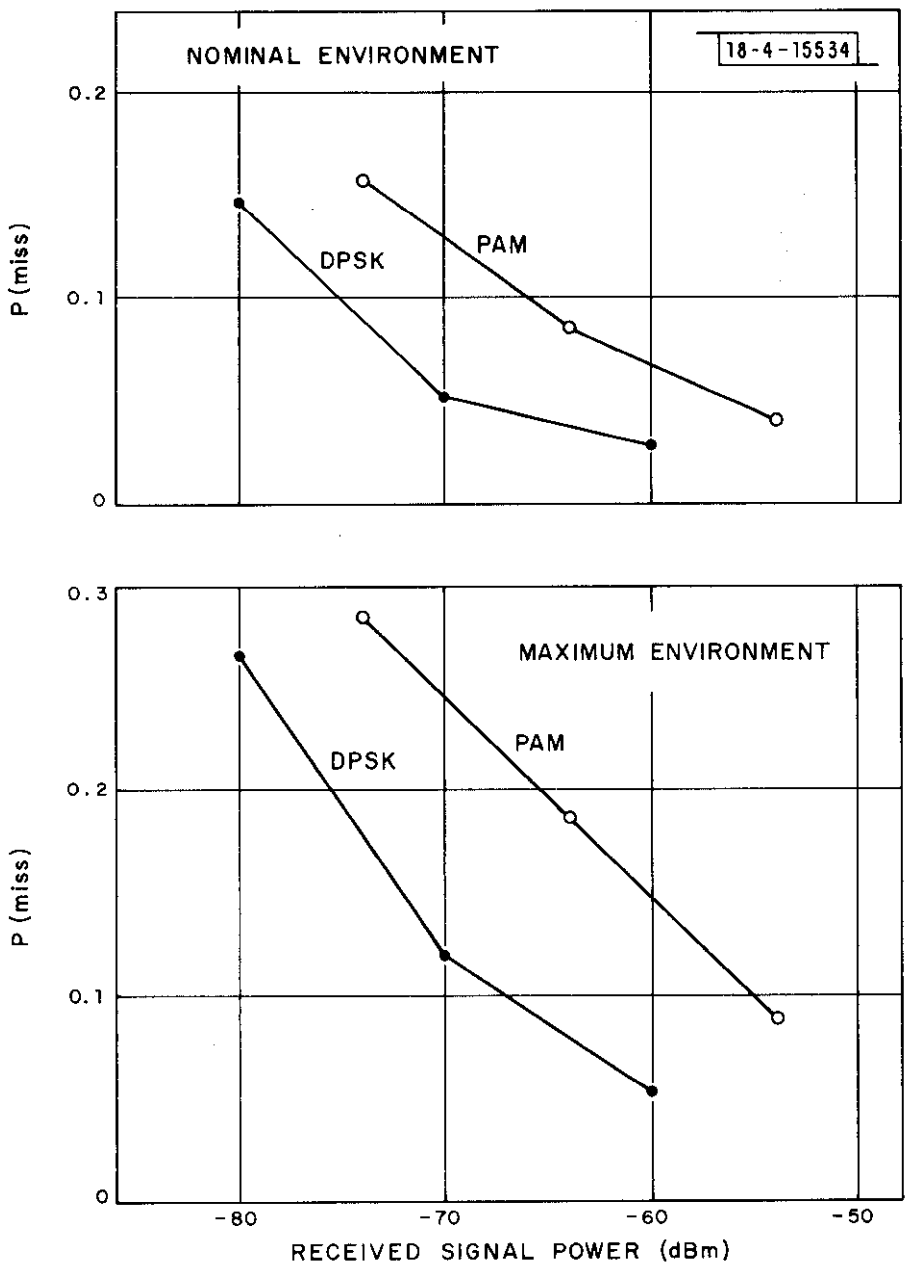

LOCATION – NEW YORK
ALTITUDE = 10,000 ft
NOISE LEVEL = −90 dBm

MATCHED FILTER DEMODULATORS
PAM THRESHOLD = −4 dB
τ = 0.8 μsec
CHIP DURATION = 0.25 μsec
n = 100 bits

Fig. 5. Dependence on Signal Power.

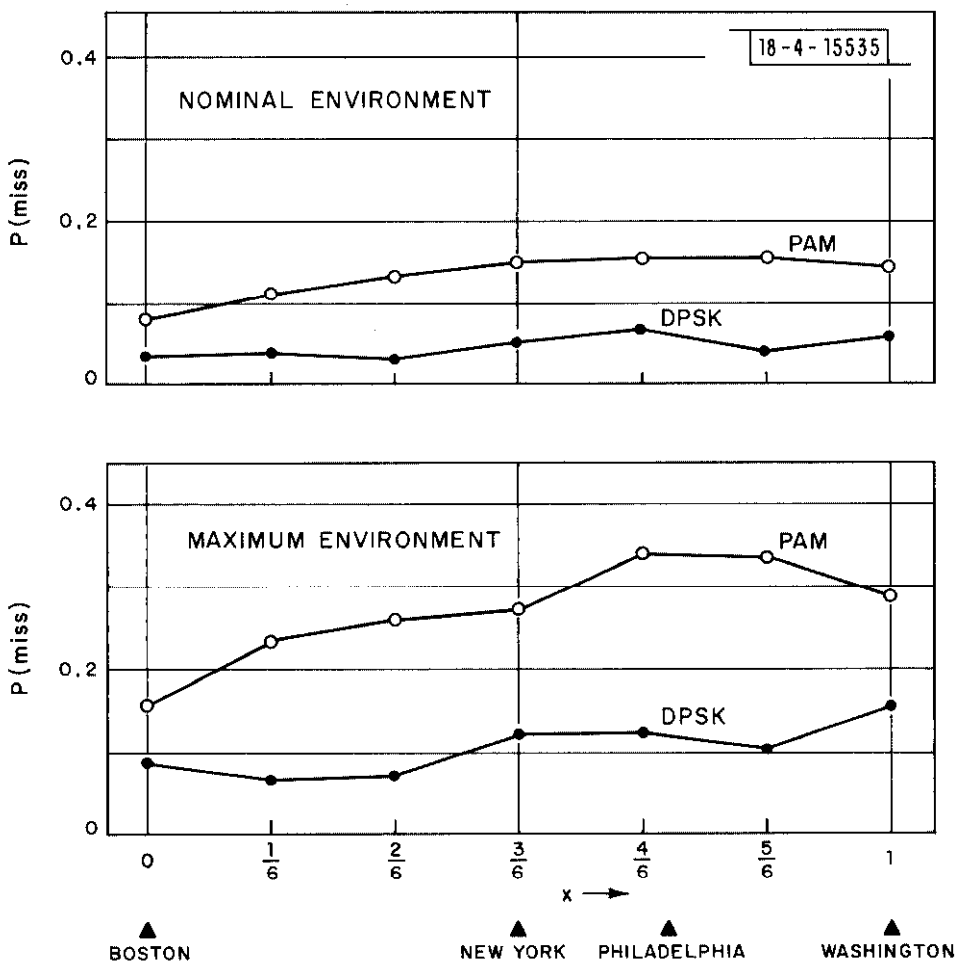

SIGNAL LEVEL = −70 dBm
SNR = 20 dB-DPSK, 26 dB-PAM
ALTITUDE = 10,000 ft

MATCHED FILTER DEMODULATORS
PAM THRESHOLD = −4 dB
τ = 0.8 μsec
CHIP DURATION = 0.25 μsec
n = 100 bits

Fig. 6. Geographical Dependence.

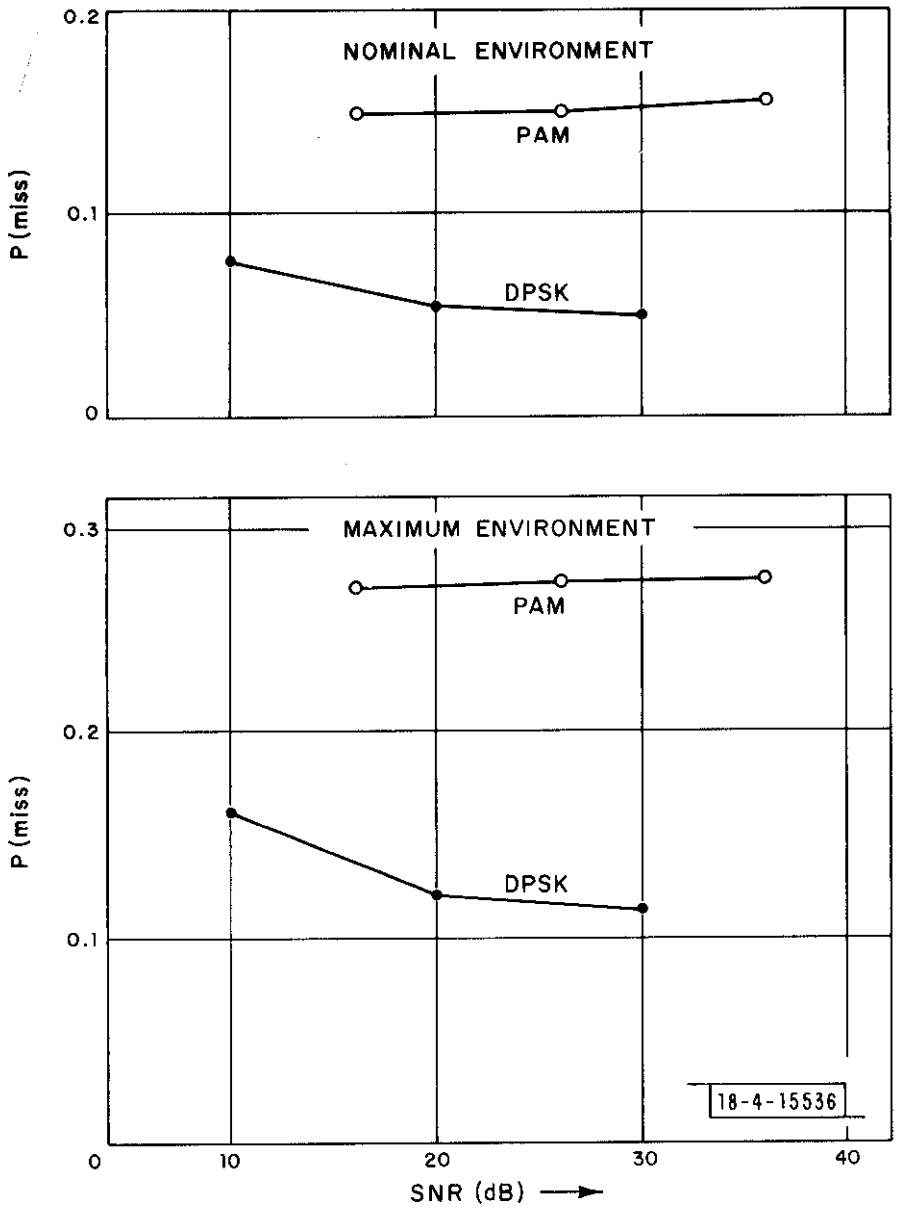

LOCATION – NEW YORK
ALTITUDE = 10,000 ft
SIGNAL LEVEL = -70 dBm

MATCHED FILTER DEMODULATORS
PAM THRESHOLD = -4 dB
τ = 0.8 μsec
CHIP DURATION = 0.25 μsec
n = 100 bits

Fig. 7. Dependence on Noise Level.

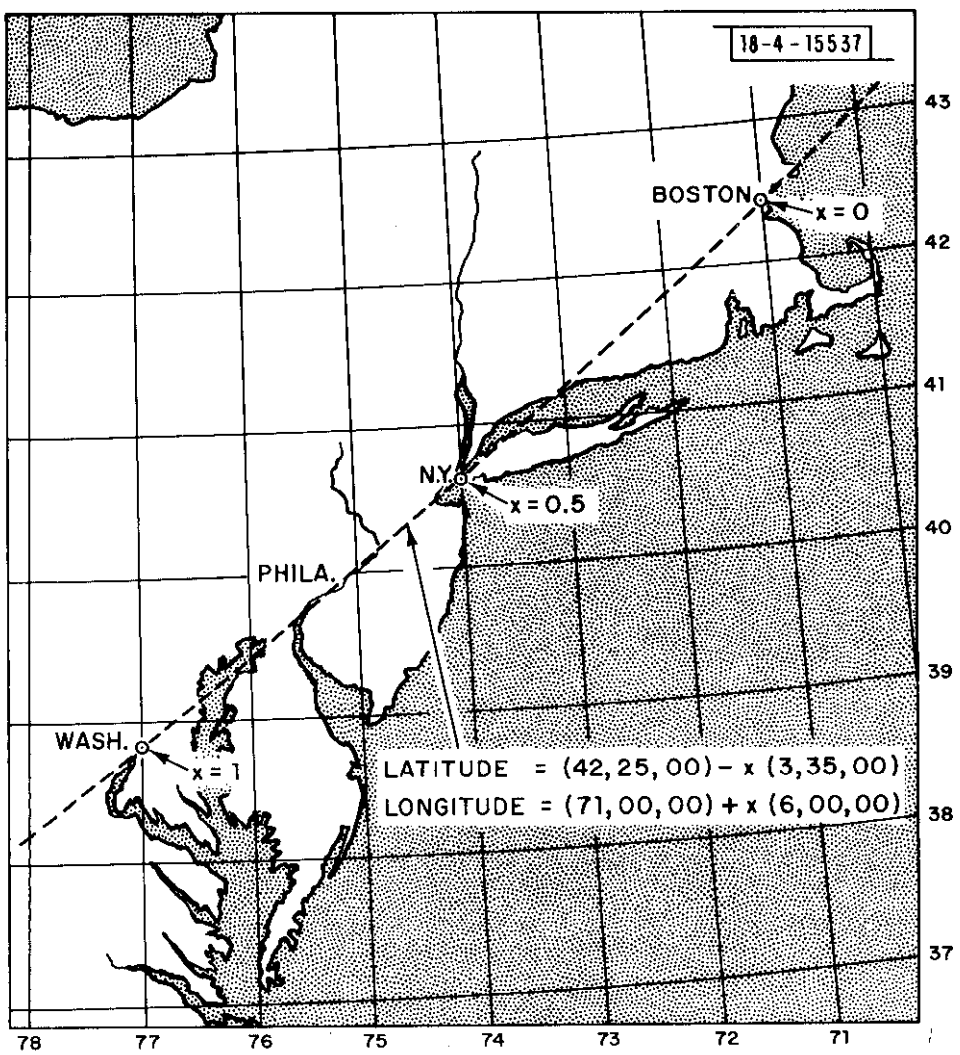

Fig. 8. Aircraft Locations Along a Boston-to-Washington Contour.

about 100 miles and thus P(miss) may receive contributions from both the New York area and the Washington area when the aircraft is located midway between. However, DPSK having a lesser range of susceptibility is more influenced by nearby interrogators, with the result being the separate peaks at Boston, New Jersey, and Washington observed in Figure 6.

3.3 Effective Interference Tolerance

The abruptness of the conditional miss curves shown in Figure 3 together with the weakness of the dependence on noise level observed in Figure 7 have suggested a simple rule of thumb to characterize the interference-error mechanism. The suggested rule is that when SIR is less than a certain level an error is always produced, and when SIR exceeds this level an error is never produced. This critical SIR level is denoted SIR_e and is assigned the values

$$SIR_e = \begin{cases} 1 \quad (\text{or } 0 \text{ dB}), & \text{DPSK} \\ \\ 4 \quad (\text{or } 6 \text{ dB}), & \text{PAM} \end{cases} .$$

This simplified behavior can be used to simplify the P(miss) formula, Eq. (T-1), by the substitutions

$$P'(M/\Omega;\ SIR,\ SNR) = u(SIR_e - SIR)$$
$$p = 0$$

where $u(\cdot)$ is the step function defined in Eq. (3-2), with the result

$$P(\text{miss}) \simeq 1 - e^{-(T_b+\tau)\ PAR(S/SIR_e)} \qquad (3\text{-}3)$$

where PAR(I) is the P_2 pulse arrival rate as defined in Eq. (3-1) and plotted in Figure 4.

To check the accuracy of this simplified formula, Figure 9 has been prepared. The graph shows P(miss) according to the simplified calculation, Eq. (3-3) plotted vs. P(miss) according to the detailed calculation, Eq. (1-1). The points plotted are all those points in Figures 5,6, and 7 at either New York, Philadelphia, or Washington. The comparison indicates a reasonable agreement, with 90% of the approximate values lying within $\pm$ 30% of the values given by the more detailed calculation.

Evidently, most of the DPSK points in Figure 9 fall above the diagonal plotted whereas most of the PAM points fall below this diagonal. This behavior indicates that DPSK is somewhat more tolerant and PAM somewhat less tolerant to interference than the amounts assumed. That is, in a complicated interference environment, DPSK is more tolerant to interference than PAM by better than 6 dB.

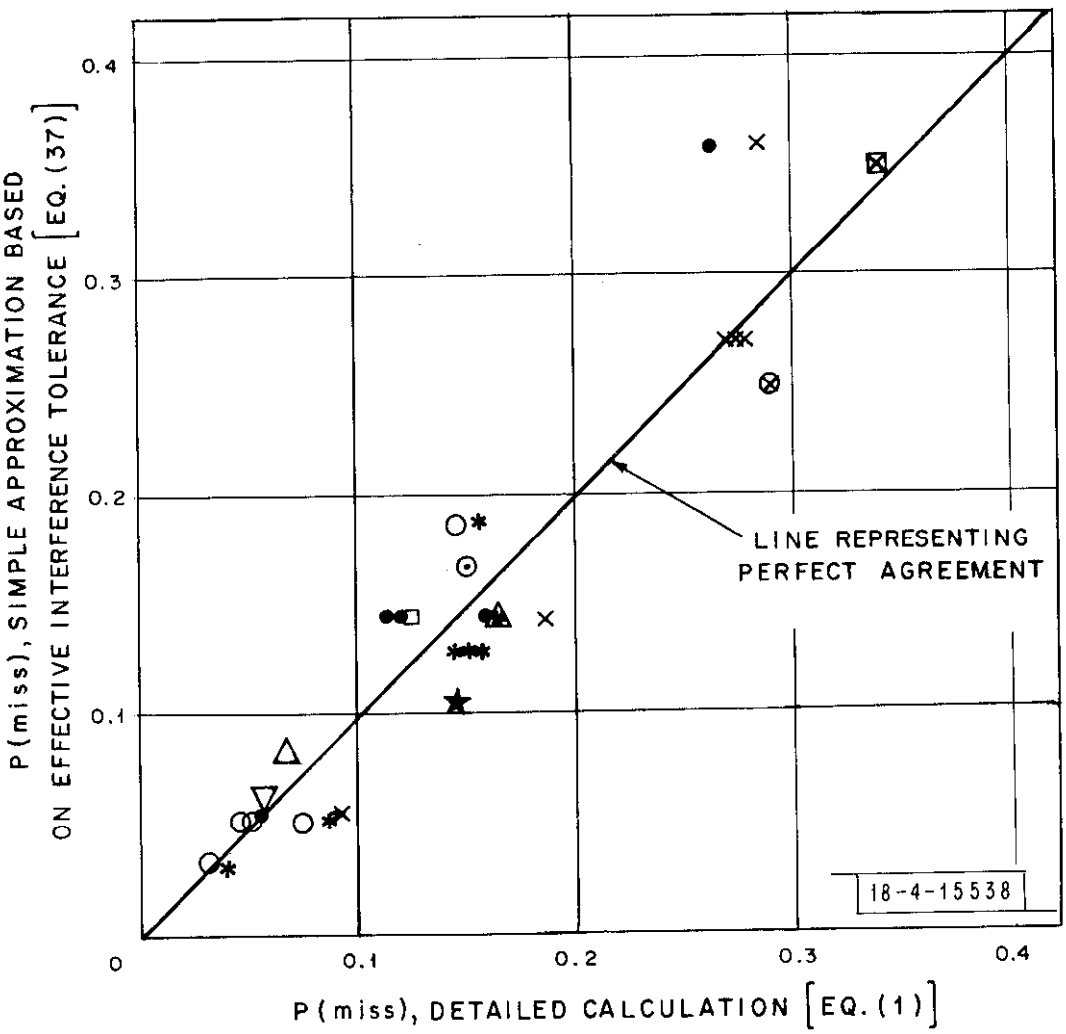

● Denotes New York, DPSK, maximum environment
× Denotes New York, PAM, maximum environment
○ Denotes New York, DPSK, nominal environment
✱ Denotes New York, PAM, nominal environment
⊙ Denotes Washington, DPSK, maximum environment
⊗ Denotes Washington, PAM, maximum environment
▽ Denotes Washington, DPSK, nominal environment
★ Denotes Washington, PAM, nominal environment
□ Denotes Philadelphia, DPSK, maximum enviornment
⊠ Denotes Philadelphia, PAM, maximum environment
△ Denotes Philadelphia, DPSK, nominal environment
⧋ Denotes Philadelphia, PAM, nominal environment

Fig. 9. A Comparison used to Assess the Validity of the Concept of "Effective Interference Tolerance."

APPENDIX A

DERIVATIONS

A.1 Derivation of Miss Probability

In deriving a formula for miss probability, it is found that several approximations are required. In order to isolate these and to give reasons for their acceptance, the derivation is divided into two parts. The first part is a special case in which noise is not present, and the second part is the more general case. Furthermore, a preliminary section of the derivation focuses attention on the relative occurrences of two types of interference overlaps, developing results that are useful in understanding the various approximations.

A.1.1 Overlap and mutual overlap

The terms "overlap" and "mutual overlap" are defined as follows:

Overlap - an event in which an interference pulse overlaps some portion of the data block.

Mutual overlap - an event in which two interference pulses both overlap to some extent the portion of signal corresponding to one bit.

In this section, formulas are developed for the average number of overlaps and the average number of mutual overlaps. For simplicity and because only the

qualitative nature of these results is to be used, attention is limited to a specific case, namely, $f_k = 0.01/(T_b + \tau)$ for all k.*

In calculating the average number of overlaps, the data block starting time is denoted as t=0. Thus, an overlap occurs if an interference pulse leading edge falls in the time interval $(-\tau, T_b)$. If A denotes the number of such pulses, then A is a random variable having a binomial distribution,

$$P(A = 0) = (1 - \alpha)^K$$

$$P(A = 1) = K\alpha(1 - \alpha)^{K-1}$$

$$P(A = 2) = \frac{1}{2} K(K - 1)\, \alpha^2(1 - \alpha)^{K-2}$$

$$\vdots$$

where $\alpha = (T_b+\tau)\, f_k = 0.01$. The mean value is

$$\bar{A} = \alpha K = \text{average number of overlaps.}$$

In calculating the average number of mutual overlaps, a specific time instant is associated with each. This time instant is taken to be at the leading edge of the later of two interference pulses which together produce the mutual overlap. In other words, a mutual overlap is said to occur at time t_o if the following conditions are all met.

(1) An interference leading edge occurs at t_o.

(2) t_o is in the interval $(-\tau, T_b)$.

(3) Another interference leading edge occurs before t_o and near enough to t_o so that one bit is affected by both pulses.

*In actuality, the repetition frequencies are deliberately made unequal, so the exact case considered in this subsection is unrealistic in this respect. However, for the purpose of estimating overlap rates, no difficulties are encountered in assuming all repetition frequencies equal, and in fact, this appears to be a reasonably accurate characterization. Since the particular value used here, $f_k = 0.01/(T_b+\tau)$, is at the upper end of allowable values, results will tend to be upper bounds rather than unbiased estimates.

In order to satisfy condition (3), the maximum separation between the two leading edges, for a given t_o, depends on the relationship between t_o and the bit structure of the data block. The maximum separation for all t_o is

$$\text{Max. separation producing mutual overlap} = t_{max} = \begin{cases} \tau + \frac{T_b}{n}, & \text{for PAM} \\ \tau + \frac{2T_b}{n+1}, & \text{for DPSK} \end{cases}$$

In the following, the occurrence of mutual overlap is overbounded (slightly) by assuming that mutual overlap always occurs when the separation is less then t_{max}.

The next step in calculating the average number of mutual overlaps is to divide up the interval $(-\tau, T_b)$ into I sub-intervals of length $\delta t = (T_b + \tau)/I$. If b_i denotes the number of mutual overlaps occurring in the i^{th} sub-interval, and B denotes the total number, then

$$B = \sum_{i=1}^{I} b_i$$

$$\bar{B} = \sum_{i=1}^{I} \bar{b}_i$$

where a bar denotes probabilistic average. When I is large and δt correspondingly small, the probability distribution of b_i is

$$P(b_i = 1) = K f_k \delta t(1 - f_k \delta t)^{K-1} \left[1 - (1 - f_k t_{max})^{K-1}\right]$$

$$P(b_i = 2) = \frac{1}{2!} K(K - 1) (f_k \delta t)^2 (1 - f_k \delta t)^{K-2} \left[1 - (1 - f_k t_{max})^{K-2}\right]$$

$$P(b_i = 3) = \frac{1}{3!} K(K - 1) (K - 2) (f_k \delta t)^3 (1 - f_k \delta t)^{K-3} \left[1 - (1 - f_k t_{max})^{K-3}\right]$$

$$\vdots$$

Therefore

$$\bar{B} = I P(b_i = 1) + 2 I P(b_i = 2) + 3 I P(b_i - 3) + \cdots$$

$$= K\alpha(1 - f_k \delta t)^{K-1} \left[1 - (1 - f_k t_{max})^{K-1}\right]$$

$$+ \frac{1}{1!} K(K - 1) \alpha(f_k \delta t) (1 - f_k \delta t)^{K-2} \left[1 - (1 - f_k t_{max})^{K-2}\right]$$

$$+ \frac{1}{2!} K(K - 1) (K - 2) \alpha(f_k \delta t)^2 (1 - f_k \delta t)^{K-3} \left[1 - (1 - f_k t_{max})^{K-3}\right]$$

$$+ \cdots$$

In the limit as $\delta t \to 0$,

$$\bar{B} = \alpha K\left[1 - \left(1 - \frac{\alpha t_{max}}{T_b + \tau}\right)^{K-1}\right]$$

These results for $\bar{A}$ and $\bar{B}$ are plotted in Figure 10 as functions of K for the case n = 100 bits and $\tau = 3T_b/n$. Mutual overlaps are seen to be much more rare than overlaps for all K values of interest.

A.1.2 Special case: Absence of noise

In this section, an expression for P(miss) is derived for the case in which noise is absent.

The derivation begins with the set equation

$$M^* = M_1^* \cap M_2^* \cap \cdots \cap M_k^* \qquad \text{(A-1)}$$

where M is the event of a miss, M_k is the event in which the k^{th} interferer acting alone produces an error, and an asterisk denotes complement. This equation is not exact, depending on mutual overlap as shown in Table A-1.

Table A.1. Dependence of Eq. (A-1) on Mutual Overlap.

Occurrence of Mutual Overlap	Correctness of Eq. (A-1)
Does not occur	Eq. (A-1) satisfied in all cases
Does occur	• Eq. (A-1) satisfied in some cases • Some occurrences are contained in the left and not the right • Some occurrences are contained in the right and not the left

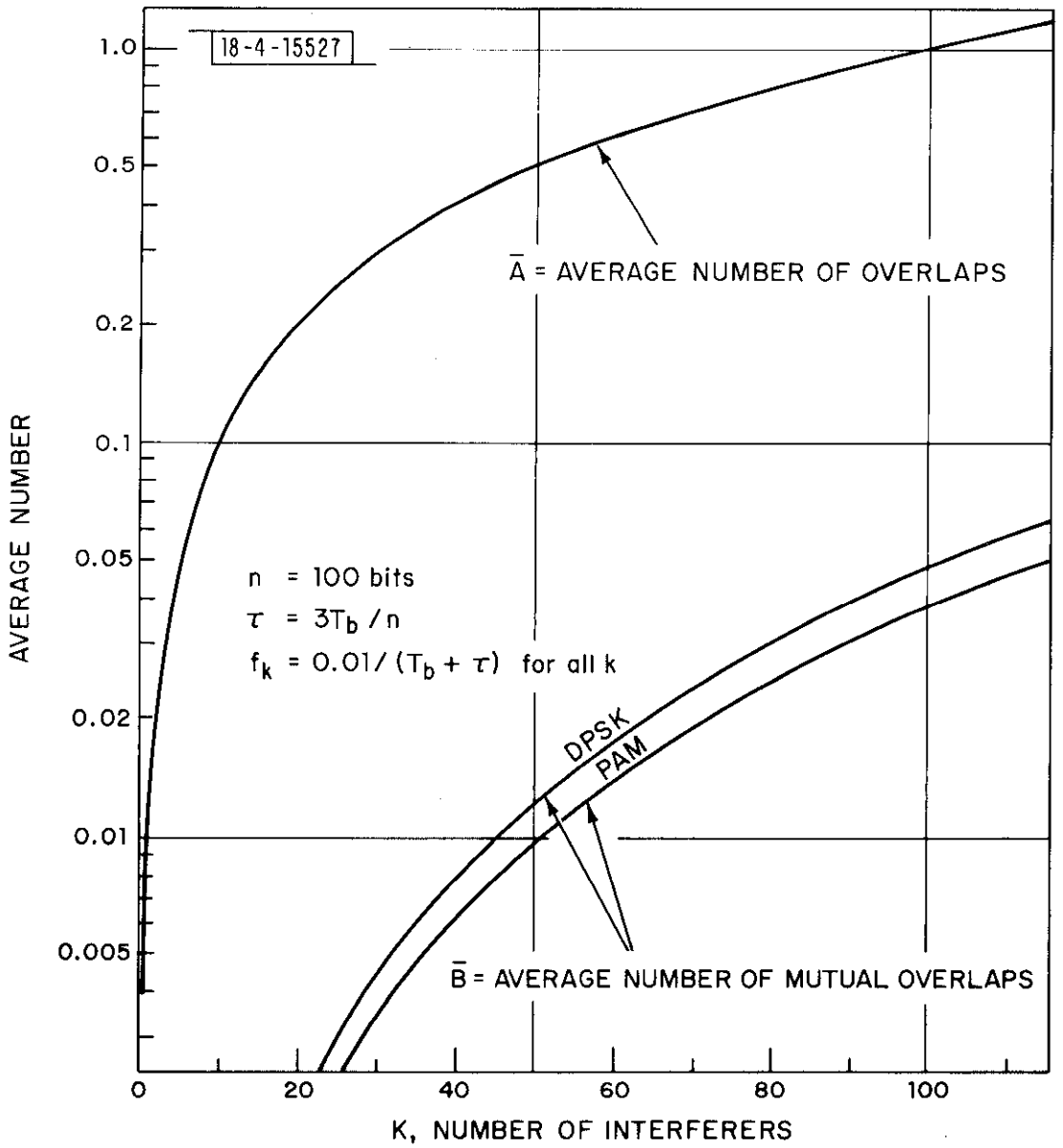

Fig. 10. Comparison Between Overlaps and Mutual Overlaps.

The argument for acceptance of Eq. (A-1) is based primarily on the relative rarity of mutual overlaps, and is strengthened somewhat by the fact that when mutual overlap does occur, the hit/miss status of the data block is often the same as would be determined by the interferers acting separately.

The next step in the derivation is the assertion

$$P(M_1^* \cap M_2^* \cap \cdots \cap M_K^*) = P(M_1^*)\, P(M_2^*) \cdots P(M_K^*) \qquad \text{(A-2)}$$

which is again an approximation felt to be very nearly exact. If the events $M_1^*, M_2^*, \cdots M_K^*$ were statistically independent, then Eq. (A-2) would, of course, be exact. However, there is a slight statistical dependence among these events. The random events $M_1^*, M_2^*, \cdots M_K^*$ have the following three sources of randomness:

(1) Carrier phases of the interferers.

(2) Pulse repetition phases of the interferers.

(3) Data-block bits.

Sources (1) and (2) cannot contribute any statistical dependence to these events, whereas source (3) can in principle. To illustrate this dependence one can consider the conditional situation in which

M_1^* -- unknown

$M_2^*, M_3^*, \cdots M_K^*$ -- known

and ask whether

$$P(M_1^*/M_2^*, M_3^*, \cdots M_K^*) \stackrel{?}{=} P(M_1^*) \qquad \text{(A-3)}$$

Conceivably, the status of M_2^*, M_3^*, $\cdots$ M_K^* may yield some hint as to the contents of the data block, and thus may change slightly the conditional probability of M_1^* so that Eq. (A-3) is not a perfect equality. This example is intended to illustrate two points: first, that there <u>is</u> in fact some degree of statistical dependence among M_1^*, M_2^*, $\cdots$ M_K^*; and second, that this dependence is extremely weak and may be neglected.

Combining Eq. (A-1) and Eq. (A-2) yields

$$P(M^*) = P(M_1^*)\, P(M_2^*) \cdots P(M_K^*)$$

which can be rewritten

$$P(M) = 1 - \prod_{k=1}^{K} [1 - P(M_k)] \quad .$$

The quantity $P(M_k)$ can be broken down into

$$P(M_k) = P(M_k/\Omega_k)\, P(\Omega_k) + P(M_k/\Omega_k^*)\, P(\Omega_k^*)$$

where Ω_k is the event that a pulse from the k^{th} interferer overlaps the signal. Since $P(M_k/\Omega_k^*) = 0$, and since $P(M_k/\Omega_k)$ depends only on SIR_k and can be written

$$P(M_k/\Omega_k) = P(M/\Omega;\ SIR_k)$$

where Ω denotes the event of exactly one overlap, and since

$$P(\Omega_k) = (T_b + \tau)\, f_k$$

the result simplifies to

$$P(M_k) = (T_b + \tau)\, f_k\, P(M/\Omega;\ SIR_k)$$

and

$$P(M) = 1 - \prod_{k=1}^{K} [1 - (T_b + \tau)\, f_k\, P(M/\Omega;\ SIR_k)] \quad . \qquad \text{(A-4)}$$

A useful simplification of this formula results from the approximation

$$1 - P(M_k) \approx e^{-P(M_k)}$$

giving the result

$$P(M) = 1 - e^{(T_b+\tau) \sum_{k=1}^{K} f_k\, P(M/\Omega;\ SIR_k)} \qquad \text{(A-5)}$$

This mathematical approximation is shown in Appendix B to introduce an inaccuracy in P(M) no larger than about 0.006 times the computed value of P(M).

Equation (A-5) is the desired result of this section. It gives miss probability in terms of interference parameters, f_1, f_2, $\cdots$ f_K and SIR_1, SIR_2, $\cdots$ SIR_K, and in terms of the conditional miss probability $P(M/\Omega;\ SIR)$. Derivation of formulas for evaluating this conditional miss probability are developed in Section A.2.

A.1.3 General case

In this section, a formula for P(miss) is derived in the more general case which includes noise as well as interference. The presence of noise can produce errors in bits not overlapped by interference and can affect the production of errors in bits that are overlapped.

Proceeding along the same lines as in the previous section, the following set equation is proposed.

$$M^* = M_n'^* \cap M_1'^* \cap M_2'^* \cap \cdots \cap M_K'^* \tag{A-6}$$

where M_n' is the event that noise produces an error in a signal bit not overlapped by interference, and M_k' is the event that a pulse from the k^{th} interferer overlaps the signal and an error is produced in one of the bits overlapped. This equation is not exact, but does hold in all cases in which mutual overlap does not occur. The argument for acceptance of Eq (A-6) is based on the relative rarity of mutual overlaps, and is strengthened somewhat by the fact that when mutual overlap does occur, the hit/miss status is often the same as would be determined by the interferers acting separately.

The next step in the derivation is the assertion

$$P(M_n'^* \cap M_1'^* \cap M_2'^* \cap \cdots \cap M_K'^*) = P(M_n'^*)\ P(M_1'^* \cap M_2'^* \cap \cdots \cap M_K'^*) \quad . \tag{A-7}$$

This is an approximation which would be exact if $M_n'^*$ and $M_1'^* \cap M_2'^* \cap \cdots M_K'^*$ were statistically independent. In fact, they are not, for the occurrence of the latter may give some hint as to the number of bits overlapped which

information would affect the conditional probability of $M_n'^*$. An explicit look at the conditional probability of $M_n'^*$, conditioned on the number of bits overlapped, namely, for any integer C (between 0 and n)

$$P(M_n'^*/c = C) = (1 - p)^{n-C}$$

where

c = number of bits overlapped, a random variable

p = bit error probability in noise alone

indicates that this probability is only weakly dependent on the number of bits overlapped in all cases of reasonable likelihood, i.e., those in which $C << n$. Because of the weakness of this dependence, and because of the additional weakness of the dependence between c and $M_1'^* \cap M_2'^* \cap \cdots \cap M_K'^*$, it is concluded that Eq. (A-7) is quite accurate. Furthermore, for the same reason we can reasonably approximate

$$P(M_n'^*) = (1 - p)^n \quad . \tag{A-8}$$

The next step in the derivation is the statement

$$P(M_1'^* \cap M_2'^* \cap \cdots \cap M_K'^*) = P(M_1'^*)\, P(M_2'^*) \cdots P(M_K'^*) \tag{A-9}$$

again an approximation claimed to be very nearly exact. The sources of randomness affecting the events involved are:

(1) Carrier phases of the interferers.

(2) Pulse repetition phases of the interferers.

(3) The noise waveform.

(4) Data-block bits.

Of these, only the 4th can contribute statistical dependence to $M_1'^*$, $M_2'^*$, ... $M_K'^*$, and for the same reasons considered in the previous section, this dependence is concluded to be extremely weak. It follows that Eq. (A-9) is an accurate approximation.

Combining Equations (A-6), (A-7), (A-8), and (A-9) leads to

$$P(M) = 1 - (1 - p)^n \prod_{k=1}^{K} [1 - P(M_k')]$$

the quantity $P(M_k')$ can be broken down into

$$P(M_k') = P(M_k'/\Omega_k)\, P(\Omega_k) + P(M_k'/\Omega_k^*)\, P(\Omega_k^*) \quad .$$

Using

$$P(M_k'/\Omega_k^*) = 0$$

$$P(\Omega_k) = (T_b + \tau)\, f_k$$

and denoting

$$P(M'_k/\Omega_k) = P'(M/\Omega;\ SIR_k,\ SNR)$$

leads to

$$P(M) = 1 - (1 - p)^n \prod_{k=1}^{K} [1 - (T_b + \tau)\ f_k\ P'(M/\Omega;\ SIR_k,\ SNR)] \quad .$$

By means of the exponential approximation discussed in the preceding section and in Appendix B, the result becomes

$$P(M) = 1 - (1 - p)^n\ e^{-(T_b+\tau) \sum_{k=1}^{K} f_k\ P'(M/\Omega;\ SIR_k,\ SNR)} \quad .$$

This equation is the desired result of this section and is the same as Eq. (1-1) given in the summary, Section 1.2. Miss probability is expressed as a function of the interference parameters f_1, f_2, ... f_K and SIR_1, SIR_2, ... SIR_K and of the conditional miss probability $P'(M/\Omega;\ SIR,\ SNR)$. Formulas for evaluating this conditional miss probability are derived in the next section.

A.2 Derivation of Conditional Probability of Miss

In this section we determine, for both DPSK and PAM, expressions for $P'(M/\Omega;\ SIR,\ SNR)$. The determination is carried out for non-coherent matched filter demodulators and for the specific case

P_2-pulse duration, $\tau = 0.8$ μsec

chip duration, $T = 0.25$ μsec .

We simplify our notation in this section by using $\rho = 1/\sqrt{SIR}$ and $\gamma = \sqrt{SNR}$. Because of their relative durations, an interference pulse will overlap up to 4 or 5 chip intervals, as is seen in the examples of Figure 11. A minimum of two and a maximum of 3 chip intervals have been completely overlapped and the remainder are only partially overlapped. We first derive an expression for Pe/bit in interference and use this in expressing $P'(M/\Omega;\ 1/\rho^2, \gamma^2)$. The resulting expressions are computationally very complicated so approximations are used for the purpose of obtaining numerical values.

A.2.1 DPSK

The expression for the DPSK bit error probability can be determined from the results of Stein (Ref. [5]) in terms of γ, ρ_1, ρ_2, and θ, where ρ_1 and ρ_2 are the interference-to-signal ratios for the first and second pulses used in the decision process and θ is the relative carrier phase difference between the signal and interference pulse. As derived in Appendix A of Ref. [6] we obtain for the bit error probability

$$P_e(\gamma,\ \rho_1, \rho_2, \theta) = \frac{1}{2}[1 - Q(\sqrt{b},\ \sqrt{a}) + Q(\sqrt{a},\ \sqrt{b})] \qquad \text{(A-10)}$$

where

$$a = 2\ \gamma^2 \left(\frac{\rho_1 - \rho_2}{2}\right)^2 \qquad \text{(A-11)}$$

and

$$b = 2\ \gamma^2 \left[1 + 2\left(\frac{\rho_1 + \rho_2}{2}\right)\cos\ \theta + \left(\frac{\rho_1 + \rho_2}{2}\right)^2\right] \qquad \text{(A-12)}$$

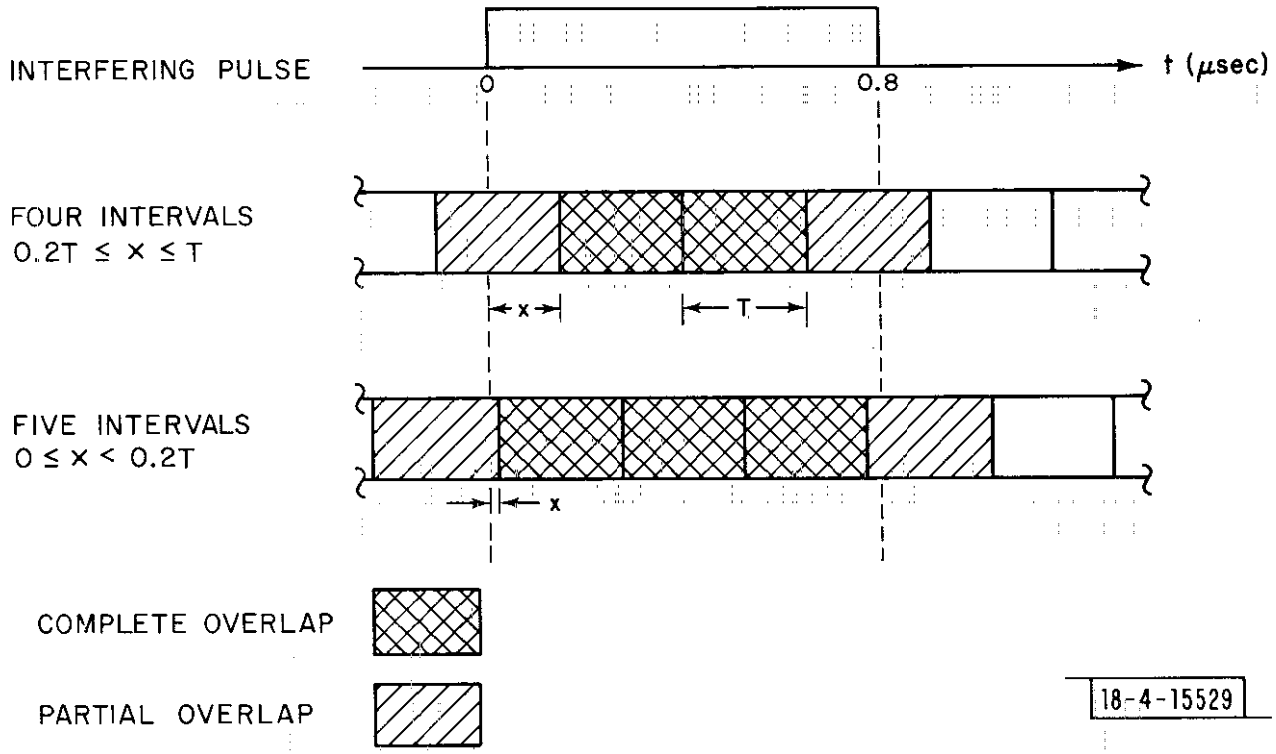

Fig. 11. The Timing Relationships Between the Interfering P_2 Pulse and the DABS Uplink Signal.

In order to proceed from bit error rates to $P'(M/\Omega;\ 1/\rho^2,\ \gamma^2)$ we must introduce the parameter x shown in Figure 11. x tells us the relative position of the interference and information pulse. As x varies, then ρ_1 or ρ_2 can change as well as the number of bits with interference. Since the error is periodic with x (ignoring the end effects of the block) with period T we can consider x uniformly distributed between 0 and T. Let τ_0/T be the fraction of signal pulse overlapped by the interfering pulse, then the effective interference-to-signal ratio, ρ', is

$$\rho' = \sqrt{\frac{\tau_0}{T}}\ \rho\ , \tag{A-13}$$

where

$$\tau_0 = \begin{cases} x & \text{for 1st interfered chip} \\ 0.2T-x & \text{for last interfered chip if } 0 \leq x < 0.2T \\ 1.2T-x & \text{for last interfered chip if } 0.2T \leq x < T \\ T & \text{for all other interfered chips} \end{cases} \tag{A-14}$$

We now use Eq. (A-10) together with Eq. (A-13) and Eq. (A-14) to express the probability of error in terms of x and to obtain $P'(M/\Omega;\ 1/\rho^2,\ \gamma^2)$ by averaging over x. Since the results are symmetrical about x = 0.6T we can integrate from x = 0.1T to x = 0.6T and double the result. The integrals become

$$P'(M/\Omega;\ 1/\rho^2,\gamma^2)$$

$$= 2\int_{0.1T}^{0.2T}\left\{1 - \frac{1}{2\pi}\int_{-\pi}^{\pi}\left[1 - \frac{1}{2}\left|P_e(\gamma,\rho,\rho,\theta) + P_e(\gamma,\rho,-\rho,\theta)\right|\right]^2\right.$$

$$\times\left[1 - \frac{1}{2}\left|P_e\left(\gamma,\rho,\sqrt{\frac{x}{T}}\,\rho,\theta\right) + P_e\left(\gamma,\rho,-\sqrt{\frac{x}{T}}\,\rho,\theta\right)\right|\right]$$

$$\times\left[1 - \frac{1}{2}\left|P_e\left(\gamma,\rho,\sqrt{\frac{0.2T-x}{T}}\,\rho,\theta\right) + P_e\left(\gamma,\rho,-\sqrt{\frac{0.2T-x}{T}}\,\rho,\theta\right)\right|\right]$$

$$\left.\times\left[1 - P_e\left(\gamma,\sqrt{\frac{x}{T}}\,\rho,0,\theta\right)\right]\left[1 - P_e\left(\gamma,\sqrt{\frac{0.2T-x}{T}}\,\rho,0,\theta\right)\right]d\theta\right\}\frac{1}{T}\,dx$$

$$+ 2\int_{0.2T}^{0.6T}\left\{1 - \frac{1}{2\pi}\int_{-\pi}^{\pi}\left[1 - \frac{1}{2}\left|P_e(\gamma,\rho,\rho,\theta) + P_e(\gamma,\rho,-\rho,\theta)\right|\right]\right.$$

$$\times\left[1 - \frac{1}{2}\left|P_e\left(\gamma,\rho,\sqrt{\frac{x}{T}}\,\rho,\theta\right) + P_e\left(\gamma,\rho,-\sqrt{\frac{x}{T}}\,\rho,\theta\right)\right|\right]$$

$$\times\left[1 - \frac{1}{2}\left|P_e\left(\gamma,\rho,\sqrt{\frac{1.2T-x}{T}}\,\rho,\theta\right) + P_e\left(\gamma,\rho,-\sqrt{\frac{1.2T-x}{T}}\,\rho,\theta\right)\right|\right]$$

$$\left.\times\left[1 - P_e\left(\gamma,\sqrt{\frac{x}{T}}\,\rho,0,\theta\right)\right]\left[1 - P_e\left(\gamma,\sqrt{\frac{1.2T-x}{T}}\,\rho,0,\theta\right)\right]d\theta\right\}\frac{1}{T}\,dx$$

(A-15)

Since Eq. (A-15) is so complicated, we approximate the result by evaluating the integrand at only two values of x (x = 0.1T and 0.6T) and averaging. The error is not great since the integrand is not very sensitive with respect to x.

A.2.2 PAM

We can handle $P'(M/\Omega;\ 1/\rho^2,\gamma^2)$ for PAM in a fashion analogous to that for DPSK except that (i) there is an additional variable v_o, the threshold parameter, and (ii) decisions are made using only a single chip. If we use α to denote the ratio of the actual threshold level to the noise- and interference-free sampled output of the receiver then we define v_o as

$$v_o = \alpha\gamma\sqrt{2} \quad . \tag{A-16}$$

In terms of v_o, the expression for the probability of error per bit is (Ref. [3])

$$P'(\gamma,\rho,\theta) = \frac{1}{2}\left[Q(\rho\sqrt{2}\ \gamma, v_o) + 1 - \frac{1}{2\pi}\int_{-\pi}^{\pi} Q(R[\rho,\theta],\ v_o)\ d\theta\right] \tag{A-17}$$

where

$$R[\rho,\theta] = \sqrt{2\ \gamma^2(1 + 2\rho\cos\theta + \rho^2)} \quad . \tag{A-18}$$

The value for the threshold which will be used in our evaluation is

$$v_o = 0.6310\ \sqrt{2}\ \gamma \qquad \text{(corresponding to -4 dB)} \tag{A-19}$$

since this results in a lower error probability in large interference than the normally used value of $\frac{1}{2}\sqrt{2}\,\gamma$ (-6 dB).

For PAM, $P'(M/\Omega;\ 1/\rho^2,\gamma^2)$ becomes

$$P'(M/\Omega;\ 1/\rho^2,\gamma^2)$$

$$= 2\int_{0.1T}^{0.2T}\left\{1 - \frac{1}{2\pi}\int_{-\pi}^{\pi}\left[1 - \frac{1}{2}\left|Q(\rho\sqrt{2}\,\gamma,v_o) + 1 - Q(R[\rho,\theta],v_o)\right|\right]^3\right.$$

$$\times\left[1 - \frac{1}{2}\left|Q\left(\rho\sqrt{2\tfrac{x}{T}}\,\gamma,v_o\right) + 1 - Q\left(R\left[\sqrt{\tfrac{x}{T}}\,\rho,\theta\right],v_o\right)\right|\right]$$

$$\left.\times\left[1 - \frac{1}{2}\left|Q\left(\rho\sqrt{2\tfrac{0.2T-x}{T}}\,\gamma,v_o\right) + 1 - Q\left(R\left[\sqrt{\tfrac{0.2T-x}{T}}\,\rho,\theta\right],v_o\right)\right|\right]d\theta\right\}\frac{1}{T}dx$$

$$+ 2\int_{0.2T}^{0.6T}\left\{1 - \frac{1}{2\pi}\int_{-\pi}^{\pi}\left[1 - \frac{1}{2}\left|Q(\rho\sqrt{2}\,\gamma,v_o) + 1 - Q(R[\rho,\theta],v_o)\right|\right]^2\right.$$

$$\times\left[1 - \frac{1}{2}\left|Q\left(\rho\sqrt{\tfrac{2x}{T}}\,\gamma,v_o\right) + 1 - Q\left(R\left[\sqrt{\tfrac{x}{T}}\,\rho,\theta\right],v_o\right)\right|\right]$$

$$\left.\times\left[1 - \frac{1}{2}\left|Q\left(\rho\sqrt{2\tfrac{1.2T-x}{T}}\,\gamma,v_o\right) + 1 - Q\left(R\left[\sqrt{\tfrac{1.2T-x}{T}}\,\rho,\theta\right],v_o\right)\right|\right]d\theta\right\}\frac{1}{T}dx$$

(A-20)

Again, we simplify the computation by averaging over two values of x(x=0.1T and x=0.6T) instead of integrating.

A.2.3 Special case: Absence of noise

At infinite signal-to-noise ratio, we can obtain alternate expressions for $P'(M/\Omega;\ 1/\rho^2,\infty)$. These can then be compared to our previous expressions with large γ as well as provide us with the asymptotes. The bit error probabilities for DPSK are determined with the aid of Figure 12. We have that

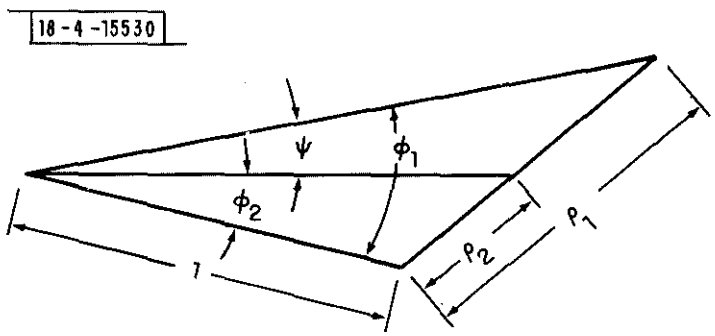

Figure 12. Normalized Phasor Diagram for DPSK.

$$\phi_1 = \tan^{-1} \frac{\rho_1 \sin \theta}{1 + \rho_1 \cos \theta} \qquad \text{(A-21)}$$

and

$$\phi_2 = \tan^{-1} \frac{\rho_2 \sin \theta}{1 \pm \rho_2 \cos \theta} \qquad \text{(A-22)}$$

where the minus would apply when the phase of the 2nd signal chip differed from that of the first. From Eq. (A-21) and Eq. (A-22) we obtain

$$\cos \phi_1 = \frac{1 + \rho_1 \cos \theta}{\sqrt{1 + 2 \rho_1 \cos \theta + \rho_1^2}} , \sin \phi_1 = \frac{\rho_1 \cos \theta}{\sqrt{1 + 2 \rho_1 \cos \theta + \rho_1^2}}$$

(A-23)

and

$$\cos \phi_2 = \frac{1 \pm \rho_2 \cos \theta}{\sqrt{1 \pm 2 \rho_2 \cos \theta + \rho_2^2}} , \sin \phi_2 = \frac{\rho_2 \cos \theta}{\sqrt{1 \pm 2 \rho_2 \cos \theta + \rho_2^2}}$$

(A-24)

which yields

$$\cos \psi = \cos(\phi_1 \mp \phi_2) = \frac{(1 + \rho_1 \cos \theta)(1 \pm \rho_2 \cos \theta) \pm \rho_1 \rho_2 \sin^2 \theta}{\sqrt{(1 + 2 \rho_1 \cos \theta + \rho_1^2)(1 \pm 2 \rho_2 \cos \theta + \rho_2^2)}}$$

(A-25)

or

$$\psi = \cos^{-1} \frac{1 + (\rho_1 \pm \rho_2) \cos \theta \pm \rho_1 \rho_2}{\sqrt{(1 + 2 \rho_1 \cos \theta + \rho_1^2)(1 \pm 2 \rho_2 \cos \theta + \rho_2^2)}} . \qquad \text{(A-26)}$$

An error occurs when

$$|\psi| \geq \frac{\pi}{2}$$

which from Eq. (A-26) is equivalent to

$$1 + (\rho_1 \pm \rho_2) \cos \theta \pm \rho_1\rho_2 \leq 0. \tag{A-27}$$

Solving for θ, we obtain

$$|\theta| \leq \cos^{-1}\left[- \frac{(1 \pm \rho_1\rho_2)}{\rho_1 \pm \rho_2} \right] \tag{A-28}$$

where each sign occurs with probability 1/2.

Equations (A-13) and (A-14) still apply for expressing ρ_1 and ρ_2 in terms of x. We have therefore, a per bit error probability

$$P_\infty(\rho_1,\rho_2) = \begin{cases} 0, & \dfrac{1 + \rho_1\rho_2}{\rho_1 + \rho_2} > 1 \\ \text{Prob}\left\{ -\cos^{-1}\left(\dfrac{1 + \rho_1\rho_2}{\rho_1 + \rho_2}\right) \leq \theta \leq \cos^{-1}\left(\dfrac{1 + \rho_1\rho_2}{\rho_1 + \rho_2}\right) \right\}, & -1 \leq \dfrac{1 + \rho_1\rho_2}{\rho_1 + \rho_2} \leq 1 \\ 1, & \dfrac{1 + \rho_1\rho_2}{\rho_1 + \rho_2} < -1 \end{cases} \tag{A-29}$$

where θ is uniformly distributed between $-\pi$ and π. Using Eq. (A-29) we must take into account the fact that θ is dependent from bit to bit since we are dealing with but a single interference pulse. We note first that for $\rho < 1$ there can be no errors. For $\rho \geq 1$ a partial overlap for ρ_2 and full overlap for ρ_1, can cause an error only when

$$\rho_2 < 1/\rho \text{ when + is used} \qquad \text{or} \qquad \rho_2 > 1/\rho \text{ when - is used.} \quad \text{(A-30)}$$

We have, therefore, for $1 \leq \rho \leq 2$

$$P(M/\Omega;1/\rho^2,\infty)$$

$$= 2\int_{0.1T}^{0.2T}\left\{\frac{3}{4} + \frac{1}{16}\left[P_\infty\left(\rho,\sqrt{\frac{0.2T-x}{T}}\,\rho\right) + P_\infty\left(\rho,-\sqrt{\frac{0.2T-x}{T}}\,\rho\right) + 2\,P_\infty\left(\rho,-\sqrt{\frac{x}{T}}\,\rho\right)\right]\right\}\frac{1}{T}\,dx$$

$$+ 2\int_{0.2T}^{0.6T}\left\{\frac{1}{2} - \frac{1}{8}\left[P_\infty\left(\rho,\sqrt{\frac{1.2T-x}{T}}\,\rho\right) + P_\infty\left(\rho,-\sqrt{\frac{1.2T-x}{T}}\,\rho\right) + 2\,P_\infty\left(\rho,-\sqrt{\frac{x}{T}}\,\rho\right)\right.\right.$$

$$\left.\left. + \frac{1}{2}\,P_\infty\left(0,\sqrt{\frac{1.2T-x}{T}}\,\rho\right)\right]\right\}\frac{1}{T}\,dx \qquad \text{(A-31)}$$

Similar expressions can be obtained for other ranges of ρ but it is very cumbersome to enumerate them. For any given value of x, the conditional probability, given x is easy to evaluate but the expressions change as x changes. Therefore, similar to the noisy cases we average over two values of x ($x = 0.1T$ and $0.6T$).

For PAM we have the normalized phasor diagram shown in Figure 13. We have

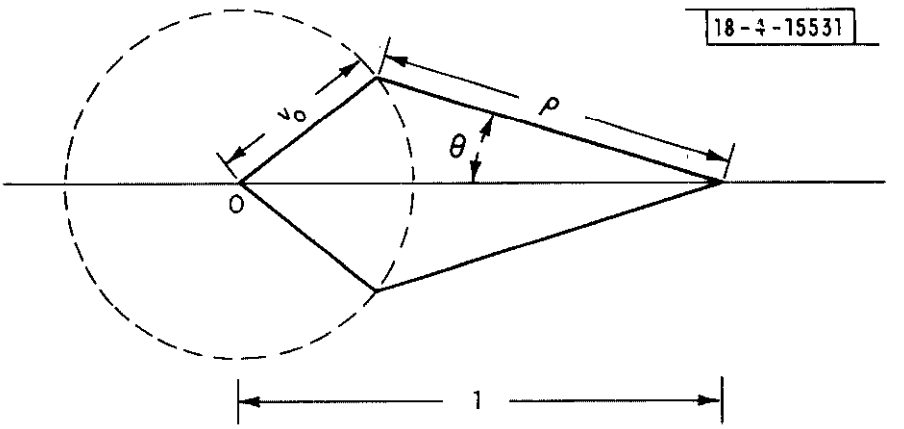

Figure 13. Normalized Phasor Diagram for PAM.

that

$$\theta = \cos^{-1}\left(\frac{\rho^2 - v_o^2 + 1}{2\rho}\right) \quad . \tag{A-32}$$

The bit error probability is seen to be for a mark

$$P_m(\rho, v_o) = \begin{cases} 0 \ , & \frac{\rho^2 - v_o^2 + 1}{2\rho} > 1 \\ \text{Prob}\left\{-\cos^{-1}\left(\frac{\rho^2 - v_o^2 + 1}{2\rho}\right) \leq \theta \leq \cos^{-1}\left(\frac{\rho^2 - v_o^2 + 1}{2\rho}\right)\right\} \ , & -1 \leq \frac{\rho^2 - v_o^2 + 1}{2\rho} \leq 1 \\ 1 \ , & \frac{\rho^2 - v_o^2 + 1}{2\rho} < -1 \end{cases} \tag{A-33}$$

where θ is uniformly distributed between $-\pi$ and π, while for a space

$$P_s(\rho,v_o) = \begin{cases} 0 & \rho < v_o \\ \\ 1 & \rho > v_o \end{cases} . \qquad \text{(A-34)}$$

It is easily seen that:

(i)	$\rho < 1 - v_o$	$P_s = 0$	$P_m = 0$
(ii)	$1 - v_o \leq \rho \leq v_o$	$P_s = 0$	$P_m \neq 0$
(iii)	$v_o < \rho < 1 + v_o$	$P_s = 1$	$P_m \neq 0$
(iv)	$\rho > 1 + v_o$	$P_s = 1$	$P_m = 0$

For $0 < \rho < \sqrt{1 + v_o^2}$ we obtain

$P'(M/\Omega;\ 1/\rho^2,\infty) =$

$$\frac{1}{5}\left\{\frac{3}{4}[1 - \{1 - P_M(\rho,v_o\}\{1 - P_s(\rho,v_o)\}] + \frac{1}{32}[P_m(\rho,v_o) + P_s(\rho,v_o)]\right\}$$

$$+ 2\int_{0.1T}^{0.2T} \frac{3}{32}\left\{\left[1-\{1-P_m(\rho,v_o)\}\left\{1-P_s\left(\sqrt{\frac{x}{T}}\,\rho.v_o\right)\right\}\right] + \left[1-\left\{1-P_m\left(\sqrt{\frac{x}{T}}\,\rho,v_o\right)\right\}\{1-P_s(\rho,v_o)\}\right]\right\}\frac{dx}{T}$$

$$+ \frac{4}{5}\left\{\frac{1}{2}[1 - \{1 - P_m(\rho,v_o)\}\{1 - P_s(\rho,v_o)\}] + \frac{1}{8}[P_m(\rho,v_o) + P_s(\rho,v_o)]\right\}$$

$$+ 2\int_{0.2T}^{0.6T} \frac{5}{16}\left\{\left[1-\{1-P_m(\rho,v_o)\}\left\{1-P_s\left(\sqrt{\frac{1.2T-x}{T}}\,\rho,v_o\right)\right\}\right] + \left[1-\left\{1-P_m\left(\sqrt{\frac{1.2T-x}{T}}\,\rho,v_o\right)\right\}\right.\right.$$

$$\left.\left.\{1-P_s(\rho,v_o)\}\right]\right\}\frac{dx}{T} \qquad \text{(A-35)}$$

Other ranges of ρ require even more complicated expression because $P_M(\rho,v_o)$ is not monotonic with ρ (See Fig. 13). $P_M(\rho,v_o)$ increases from $\rho' = 0$ to $\rho' = \sqrt{1+v_o^2}$ but decreases from its maximum at $\rho' = \sqrt{1+v_o^2}$ to zero at $\rho = 1 + v_o$. This means that fractional terms such as $\sqrt{\frac{x}{T}}\,\rho$ can cause larger error probabilities than the ρ term itself. Given any value of x, however, the conditional probability given x is straight forward and instead of obtaining the general expression we again average over the two values of x(0.1T and 0.6T).

APPENDIX B

AN EXPONENTIAL APPROXIMATION

It is to be shown that $A \approx A'$ where

$$A = 1 - \prod_{k=1}^{K} (1 - p_k)$$

$$A' = 1 - e^{-\sum_{k=1}^{K} p_k}$$

$$p_k \leq 0.01 \text{ for all } k \quad .$$

The accuracy of this approximation is being assessed here in support of statements made in Section A.1.2 and A.1.3 in Appendix A. The quantity A' is regarded as an approximation to the quantity A, used because A' is easier to calculate.

We define variables C and C' by

$$C = -\ln(1 - A)$$

$$C' = -\ln(1 - A')$$

then

$$C = -\sum_{k=1}^{K} \ln(1 - p_k)$$

$$C' = \sum_{k=1}^{K} p_k \quad .$$

Using the Taylor series

$$-\ln(1 - x) = x + x^2/2 + x^3/3 + \ldots$$

gives

$$C = \sum_{k=1}^{K} p_k + \frac{1}{2}\sum_{k=1}^{K} p_k^2 + \frac{1}{3}\sum_{k=1}^{K} p_k^3 + \ldots \quad .$$

Evidently, C' is just the first term in this expansion, and the higher-order terms are guaranteed to be small.

$$C' = C + \varepsilon$$

$$|\varepsilon| < 0.006\ C$$

This small error in C' transfers to a small error in A' by the nonlinear function, f, relating C' to A', namely

$$A' = f(C')$$

$$A = f(C)$$

$$f(x) = 1 - e^{-x}$$

The transfer is

$$A' = f(C + \varepsilon) = f(C) + \varepsilon_A = A + \varepsilon_A$$

$$\varepsilon_A \approx \varepsilon \frac{df(C)}{dc} = \varepsilon\, e^{-C}$$

$$|\varepsilon_A| \lesssim 0.006\, A\left[\frac{A - 1}{A} \ln(1 - A)\right] \quad .$$

Since for all values of A between 0 and 1, the factor in square brackets does not exceed unity, the result is

$$|\varepsilon_A| \lesssim 0.006\, A$$

or alternatively

$$|\varepsilon_A| \lesssim 0.006\, A' \quad .$$

Thus the error resulting from the use of A' as an approximation to A is not larger than about 0.006 times the computed value.

APPENDIX C

INTERPOLATION FORMULAS

The following functions are used to express the conditional probabilities of miss:

DPSK 10 dB

Range	Expression
$-\infty < \rho \leq -8$	$0.29187 \exp[0.45246\rho]$
$-8 < \rho \leq -4$	$0.85768 \exp[0.59496\rho]$
$-4 < \rho \leq -2$	$0.71631 \exp[0.54987\rho]$
$-2 < \rho \leq -1$	$0.58680 \exp[0.45015\rho]$
$-1 < \rho \leq 0$	$0.53150 \exp[0.35118\rho]$
$0 < \rho \leq 2$	$0.971875 - 0.44038 \exp[-0.42195\rho]$
$2 < \rho \leq 4$	$0.971875 - 0.35980 \exp[-0.32091\rho]$
$4 < \rho < \infty$	$0.971875 - 0.17602 \exp[-0.14217\rho]$

DPSK 20 dB

Range	Expression
$-\infty < \rho \leq -1$	$0.379702 \exp[1.8184\rho]$
$-1 < \rho \leq 0$	$0.42760 \exp[1.9372\rho]$
$0 < \rho \leq 1$	$0.971875 - 0.544275 \exp[-0.89734\rho]$
$1 < \rho \leq 2$	$0.971875 - 0.32393 \exp[-0.37839\rho]$
$2 < \rho \leq 4$	$0.971875 - 0.235738 \exp[-0.219502\rho]$
$4 < \rho < \infty$	$0.971875 - 0.168150 \exp[-0.13504\rho]$

DPSK 30 dB

Range	Expression
$-\infty < \rho \leq 0$	$0.3873 \exp[13.52474\rho]$
$0 < \rho \leq 1$	$0.971875 - 0.58458 \exp[-0.92469\rho]$
$1 < \rho \leq 2$	$0.971875 - 0.34582 \exp[-0.39971\rho]$
$2 < \rho \leq 4$	$0.971875 - 0.24325 \exp[-0.22379\rho]$
$4 < \rho < \infty$	$0.971875 - 0.17459 \exp[-0.14088\rho]$

PAM 16 dB (-4 dB threshold)

Range	Expression
$-\infty < \rho \leq -8$	$2.8686 \exp[0.3731\rho]$
$-8 < \rho \leq -6$	$3.57031 \exp[0.40046\rho]$
$-6 < \rho \leq -4$	$-0.001564\rho^4 - 0.045775\rho^3 - 0.46069\rho^2 - 1.7751\rho - 1.6037$
$-4 < \rho \leq 3$	$-0.000204\rho^4 + 0.001718\rho^3 - 0.00487\rho^2 + 0.00528\rho + 0.92607$
$3 < \rho \leq 10$	$0.00414\rho + 0.91557$
$10 < \rho < \infty$	$0.94375 + 0.01464 \exp[-0.01\rho]$

PAM 26 dB (-4dB threshold)

Range	Expression
$-\infty < \rho \leq -12$	0.0
$-12 < \rho \leq -10$	$0.017634\rho + 0.211608$
$-10 < \rho \leq -8$	$0.0240\rho + 0.2753$
$-8 < \rho \leq -4.8$	$0.023010\rho^2 + 0.351996\rho + 1.47460$
$-4.8 < \rho \leq -4$	$0.003748\rho^4 + 0.11825\rho^3 + 1.3531\rho^2 + 6.7244\rho + 12.476$

$-4 < \rho \leq -3.8$	$-0.002976\rho^4 - 0.000124\rho^3 + 0.029637\rho^2 + 0.000123\rho + 0.89934$
$-3.8 < \rho \leq -1$	$-0.03255\rho^2 - 0.07968\rho + 0.87886$
$-1 < \rho \leq 1$	0.926
$1 < \rho \leq 3$	$-0.002\rho + 0.928$
$3 < \rho \leq 10$	$0.005\rho + 0.907$
$10 < \rho < \infty$	$0.94375 + 0.0174635 \exp[-0.01\rho]$

PAM 36 dB (-4 dB threshold)

Range	Expression
$-\infty < \rho \leq -12$	0.0
$-12 < \rho \leq -10$	$0.015\rho + 0.18$
$-10 < \rho \leq -8$	$0.024\rho + 0.27$
$-8 < \rho \leq -6$	$1.01103 \exp[0.32025\rho]$
$-6 < \rho \leq -4.2$	$0.025278\rho^2 + 0.340056\rho + 1.27833$
$-4.2 < \rho \leq -4$	$1.6\rho + 7.016$
$-4 < \rho \leq -3.8$	$1.025\rho + 4.716$
$-3.8 < \rho \leq -3$	$-0.024636\rho^2 - 0.080045\rho + 0.871591$
$-3 < \rho \leq -1$	$-0.0115\rho^2 - 0.0275\rho + 0.911$
$-1 < \rho \leq 3$	$-0.0015\rho + 0.9255$
$3 < \rho \leq 10$	$0.00514\rho + 0.9056$
$10 < \rho < \infty$	$0.94375 + 0.0146435 \exp[-0.01\rho]$

REFERENCES

[1] P.R. Drouilhet, Jr., "The Development of the ATC Radar Beacon System: Past, Present, and Future," IEEE Trans. on Comm. COM-21, (May 1973), pp. 408-421.

[2] Quarterly Technical Summary, "Development of a Discrete Address Beacon System," Lincoln Laboratory, M.I.T., (1 January 1974) (in preparation).

[3] D.A. Shnidman, "A Comparison of Immunity to Garbling for Three Candidate Modulation Schemes for DABS," Lincoln Laboratory, M.I.T., Project Report ATC-12, (14 Aug. 1972) FAA-RD-72-84.

[4] Quarterly Technical Summary, "Development of a Discrete Address Beacon System," Lincoln Laboratory, M.I.T., (1 April 1973) pp. 11-13, FAA-RD-73-48.

[5] Seymour Stein, "Unified Analysis of Certain Coherent and Noncoherent Binary Communications Systems," IEEE Trans. on Info. Theory, IT-10, (January 1964), pp. 43-51.

[6] D.A. Shnidman, "The Effect of Phase Error on the DPSK Receiver Performance," Lincoln Laboratory, M.I.T., Project Report ATC-32, to be published.